Impacts of Asian megacity emissions on regional air quality during spring 2001

Sarath K. Guttikunda,[1] Youhua Tang,[2] Gregory R. Carmichael,[3] Gakuji Kurata,[2] Li Pan,[3] David G. Streets,[4] Jung-Hun Woo,[5] Narisara Thongboonchoo,[2] and Alan Fried[6]

[1] Measurements from the Transport and Chemical Evolution over the Pacific (TRACE-P) and Asian Pacific Regional Aerosol Characterization Experiment (ACE-Asia) field experiments obtained during the period of March–April 2001 are used to evaluate the impact of megacity emissions on regional air quality in east Asia. A classification method built upon back trajectory analysis and sensitivity runs using the Sulfur Transport and Emissions Model 2001 (STEM-2K1) regional chemical transport model are used to identify the aircraft observations that were influenced by megacity emissions. More than 30% of measurement points are classified as urban points, with a significant number of plumes found to have originated from Shanghai, Qingdao, Beijing, Taiyuan, Tianjin and Guiyang, Seoul, and Pusan. These data are then analyzed, and chemical characteristics of these megacities are compared. Emission estimates for the megacities are also presented and discussed in the context of expected similarities and differences in the chemical signals in the ambient air impacted by these cities. Comparisons of the observation-based ratios with emission-based estimates are presented and provide a means to test for the consistency of the emission estimates. The observation-based ratios are shown to be generally consistent with the emissions ratios. The megacity emissions are used in the STEM-2K1 model to study the effects of these emissions on criteria and photochemical species in the region. Over large portions of the Japan Sea, Yellow Sea, western Pacific Ocean, and the Bay of Bengal, megacity emissions contribute in excess of 10% of the near-surface ambient levels of O_3, CO, SO_2, H_2SO_4, HCHO, and NO_z. The megacity emissions are also used to study ozone levels in Asia under a scenario where all cities evolve their emissions in a manner such that they end up with the same VOC/NO_x emission ratio as that for Tokyo. Monthly mean ozone levels are found to increase by at least 5%.

1. Introduction

[2] In the rapidly industrializing countries the major air pollution problem has typically been high levels of smoke and SO_2 arising from the combustion of fuels for domestic and industrial activities. In both developed and developing countries, the major threat to clean air is now posed by traffic emissions, especially in the swiftly motorizing megacities of east and Southeast Asia (cities with population of 10 million or more) [*Krupnick and Harrington*, 2000; *Kojima et al.*, 2000]. Petrol- and diesel-based motor vehicles and coal combustion in the industrial boilers and power plants emit a wide variety of pollutants, viz., sulfur dioxide (SO_2), carbon monoxide (CO), nitrogen oxides (NO_x), volatile organic compounds (VOCs) and particulates. These pollutants have a significant impact on urban and regional air quality causing considerable damage to human health and ecosystems in and around the cities [*Davis et al.*, 2001]. In addition, the enhanced amounts of fine particles and photochemical oxidants observed in the urban centers have substantial potential to impact both local and regional climate [*Rotstayn et al.*, 2000]. Presently urban air pollution problems are continuing to increase and air pollutants originating from urban regions are recognized to be significantly influencing regional and global air quality [*Guttikunda*, 2002;

[1] Environment Department, World Bank, Washington, D. C., USA.
[2] Center for Global and Regional Environmental Research, University of Iowa, Iowa City, Iowa, USA.
[3] Department of Chemical and Biochemical Engineering, University of Iowa, Iowa City, Iowa, USA.
[4] Decision and Information Sciences Division, Argonne National Laboratory, Argonne, Illinois, USA.
[5] Northeast States for Coordinated Air Use Management, Boston, Massachusetts, USA.
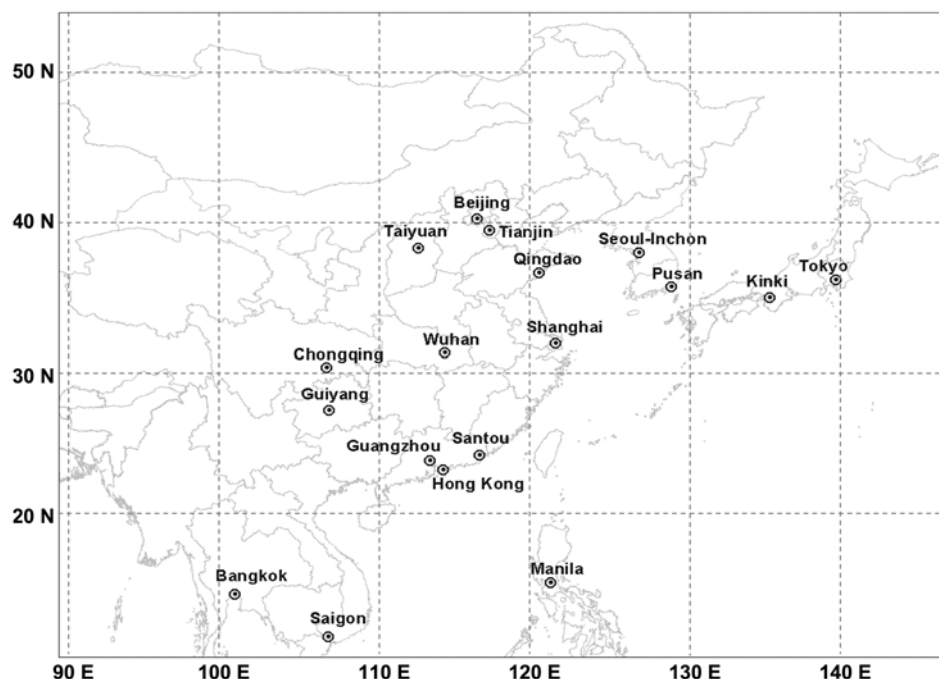[6] National Center for Atmospheric Research, Boulder, Colorado, USA.

Figure 1. Study domain and the location of megacities of Asia included in the study.

Mayer et al., 2000; *Bernsten et al.*, 1996; *Yienger et al.*, 2000].

[3] While urban environments are often the first to feel the effects of air pollution, they are also at the front line of pollution control. Significant efforts have been made during recent years to improve the urban air quality in Asia through collective efforts between government and nongovernment agencies, and international organizations. Curtailing the already substantial damage to the environment and human health and avoiding much heavier damages in the future require a thorough understanding of the urban pollution characteristics. For example, understanding the sensitivity of O_3 production to NO_x and VOC mixing ratios originating from megacities is important, because future choices need to be made as to whether the focus of pollution control efforts should be on reducing NO_x or reducing VOC emissions. The interactive nature of various pollutants and their combined effect on urban and regional air quality need to be studied before effective choices can be identified.

[4] Measurements from the Transport and Chemical Evolution over the Pacific (TRACE-P) and Asian Pacific Regional Aerosol Characterization Experiment (ACE-Asia) field experiments obtained during the period of March–April 2001 provide an opportunity to evaluate the impact of megacity emissions on regional air quality. The experiments were not designed to sample over the megacities themselves. However, the aircrafts frequently sampled plumes 0.5 to 3 days downwind of megacities in the region. In addition the detailed emissions inventory developed in support of these experiments, contained explicit information on megacities and their surrounding regions [*Streets et al.*, 2003]. With the help of analysis using a three-dimensional atmospheric chemistry model, the measurements can be used to identify and evaluate the urban characteristics. This is the subject of this paper.

[5] In this paper, we focus on (1) what the estimated emissions for the megacities in Asia tell us about the expected similarities and differences in the chemical signals in the ambient air impacted by these cities, (2) what the observed chemical signals were in megacity impacted air masses during this period, (3) an assessment of the chemical "footprint" of these megacities (i.e., the impact of these large urban sources on the pollution levels and photochemistry at downwind locations), and (4) the implications of these results with respect to possible environmental futures associated with changing megacity emissions in Asia.

2. Megacity Emissions

[6] Asian megacities are extremely diverse, with a wide variation in sources, climate, and geography. The cities included in this study are presented in Figure 1. Emission inventories for Asia developed in support of the TRACE-P and ACE-Asia experiments [*Streets et al.*, 2003] are integrated into an emission support system (ACE-Asia and TRACE-P Modeling and Emission Support System, 2001, ACE-Asia and TRACE-P modeling and emission support system, edited by G. R. Carmichael, available at http://www.cgrer.uiowa.edu/ACESS/acess_index.htm), which includes gaseous pollutants such as SO_2, NO_x, CO, and VOC, and particulate pollutants such as black carbon (BC), organic carbon (OC), and particulates (PM_{10}, with particle diameter less than 10 μm) and ($PM_{2.5}$, with particle diameter less than 2.5 μm) for Asia in the year of 2000. The data system includes information on various emission sources, compiled by region, by fuels and by economic sector, and also includes natural emission sources such as volcanoes and forest fires [*Woo et al.*, 2003]. In the developing countries, availability of local and process-specific information on emissions is one of the most serious data gaps.

Table 1. Primary Emission Estimates for the Cities of Asia in 2000[a]

	SO_2	NO_x[b]	VOC	CO	BC	OC	PM_{10}	$PM_{2.5}$
East Asia								
Beijing	238.0	118.1	225.6	1237.0	8.6	13.1	83.2	42.7
Taiyuan	178.3	52.1	55.5	329.6	4.0	3.8	28.5	11.0
Tianjin	200.7	152.6	198.8	973.1	8.1	12.8	70.4	35.7
Shanghai	250.8	222.4	348.3	1716.1	7.6	11.8	79.9	42.6
Qingdao	23.9	17.1	27.8	148.9	1.2	3.9	11.5	9.5
Guangzhou	97.2	63.3	120.0	390.6	2.7	7.5	29.6	20.9
Wuhan	93.9	56.3	115.8	594.9	10.3	30.4	95.2	73.7
Chongqing	150.5	31.9	83.3	463.4	7.8	24.4	71.4	58.1
Hong Kong	36.1	99.8	133.1	270.5	1.3	2.5	17.2	12.1
Seoul	309.9	400.9	282.1	254.1	7.0	9.0	46.9	24.0
Pusan	55.7	97.3	183.0	133.6	1.0	0.8	13.3	6.6
Tokyo	112.3	276.2	414.5	461.1	5.7	6.5	31.7	18.3
Osaka	83.1	176.7	197.6	330.2	4.1	4.7	24.3	14.9
Southeast Asia								
Bangkok	162.4	58.2	235.6	213.2	3.9	15.5	67.5	55.5
Singapore	188.7	213.7	153.7	158.2	3.9	5.1	266.0	165.4
Jakarta	97.4	66.6	671.3	1210.1	21.2	102.8	298.4	281.6
Manila	113.4	26.0	123.7	59.0	2.9	12.0	39.5	35.8
Kuala Lumpur	54.3	48.2	157.6	101.9	1.8	5.8	30.0	20.4
South Asia								
Calcutta	65.2	61.6	233.0	631.3	16.1	76.7	345.3	273.0
New Delhi	69.7	64.6	181.8	598.8	7.4	32.4	223.2	152.3
Bombay	46.3	24.8	61.0	113.4	3.0	12.8	59.5	43.5
Karachi	155.1	25.0	40.7	47.9	4.4	18.5	95.2	72.1
Lahore	93.2	32.4	88.8	254.3	6.4	28.4	155.5	117.3
Dhaka	20.3	14.1	73.5	380.5	6.3	30.9	118.3	100.2

[a]Values are in kT.
[b]NO_x emissions are given as NO_2.

Further advancement in the emission estimation and validation process enhances our understanding of megacity contribution to overall air quality. The evaluation of the emission inventories utilized in this study against the data collected during the TRACE-P and ACE-Asia field experiments is presented by *Carmichael et al.* [2003b] and *Streets et al.* [2003].

[7] City specific emission estimates are presented in Table 1. Of the total anthropogenic emissions in Asia, megacities account for 13% of SO_2 (5.5 Tg SO_2/year), 12% of NO_x (3.3 Tg NO_2/yr), 11% of CO (18.7 Tg CO/yr) (excluding biomass burning emissions), 13% of VOCs (6.68 Tg C/yr), 13% of BC (0.26 Tg C/yr) (excluding biomass burning emissions), 14% of OC (1.0 Tg C/yr) (excluding biomass burning emissions), 16% of PM_{10} (4.4 Tg PM/yr) and $PM_{2.5}$ (3.4 Tg PM/yr) in the base year 2000. While the megacity emissions account for 10–15% of total Asian anthropogenic emissions, they are concentrated into ∼2% of the land area, leading to a very high emission density. Furthermore, 30% of the Asian population resides in these cities; thus megacity emissions project a disproportionate impact on human health. The geographical location of these cities, most of which are coastal cities, plays an important role in determining how the pollutants are dispersed.

[8] The group of cities selected in this study range from cities dominated by transport related emissions (e.g., Tokyo, Seoul, Shanghai) to cities with coal-based technologies (e.g., Beijing and Dhaka). Figure 2 presents the sectoral contribution to various pollutant emissions.

[9] For SO_2, industry (IND) and power generation (PG) account for ∼80% of the emissions in Asian cities. Tokyo, Osaka and Pusan are the exceptions. Pusan is the only city with >40% of the SO_2 emissions originating from the transport sector (TRAN). This is primarily due to the use of high-sulfur diesel for shipping and road transport. Otherwise, TRAN contributes less than 5% to the SO_2 emission inventory in Asian cities.

[10] For NO_x, IND, PG and TRAN dominate the inventory, with the transport sector accounting for as much as 60% in Pusan, Tokyo and Singapore.

[11] For CO, IND and TRAN dominate the inventory, with domestic biofuels (DOMB) contributing significantly in the rural areas of Southeast and south Asia. Here the domestic sector consists of residential fuel usage and is divided into two parts: emissions due to biofuel usage (DOMB) and emissions due to fossil fuel usage (DOMF). While most of the east Asian cities have >50% of their CO emissions originating from TRAN, Hong Kong and Singapore have TRAN contributions approaching 100%.

[12] For carbonaceous particles, domestic fossil (DOMF) for the BC, and DOMB for OC, are dominant sources. TRAN is important in the northeast Asian cities and IND is important in China.

[13] For NMVOC emissions, IND and TRAN are important in the cities of China, and IND, TRAN and DOMF are important in the northeast Asian Cities. Besides industrial activity and evaporative sources, domestic coal and biofuel combustion contribute to NMVOC emissions in many Asian cities.

[14] On a broader perspective, biomass burning contributes between 10–20% of the primary trace gas and carbonaceous emissions in Asia megacities.

[15] The ratios of primary species as determined using the emission estimates for each city are presented in Table 2 and Figure 3. Differences in the primary energy mix in Asian cities are partially explained by the endowment of energy resources. Asia has 33% of world coal reserves, sufficient for more than 100 years of consumption, and these reserves are highly concentrated in China, India and Indonesia. Hence the high dependency on coal as a primary energy source in the power, industrial and domestic sectors. Use of locally available high-sulfur coal for domestic cooking and heating, small-scale industrial boilers and power sector is the main reason why the SO_2 to NO_x emission ratios are high in cities in China, Southeast Asia, and the Indian subcontinent. In China, the SO_2 to NO_x emission ratios range from ∼1.1 in Shanghai to ∼4.7 in Chongqing. In Southeast Asia this ratio ranges from ∼0.9 in Singapore to ∼4.3 in Manila, while in south Asia they vary from ∼1.0 in Calcutta and Delhi to ∼6.2 in Karachi. This wide range of values reflects cities with energy reforms in transition and a breadth of sulfur control programs. Because of an aggressive shift in the energy mix from coal to oil and gas in South Korea and Japan, implementation of strict sulfur control technologies, and a relatively higher level of vehicular emissions (especially NO_x), cities in these countries have a lower SO_2 to NO_x emission ratio (∼0.5). In the future, rapidly motorizing cities in China and the Indian Subcontinent are expected to see their SO_2 to NO_x emission ratios decrease.

[16] The VOC to NO_x emission ratios (mass based) range from ∼10 in Jakarta to ∼0.7 in Seoul. The highly motorized cities like Seoul, Tokyo, Singapore and cities
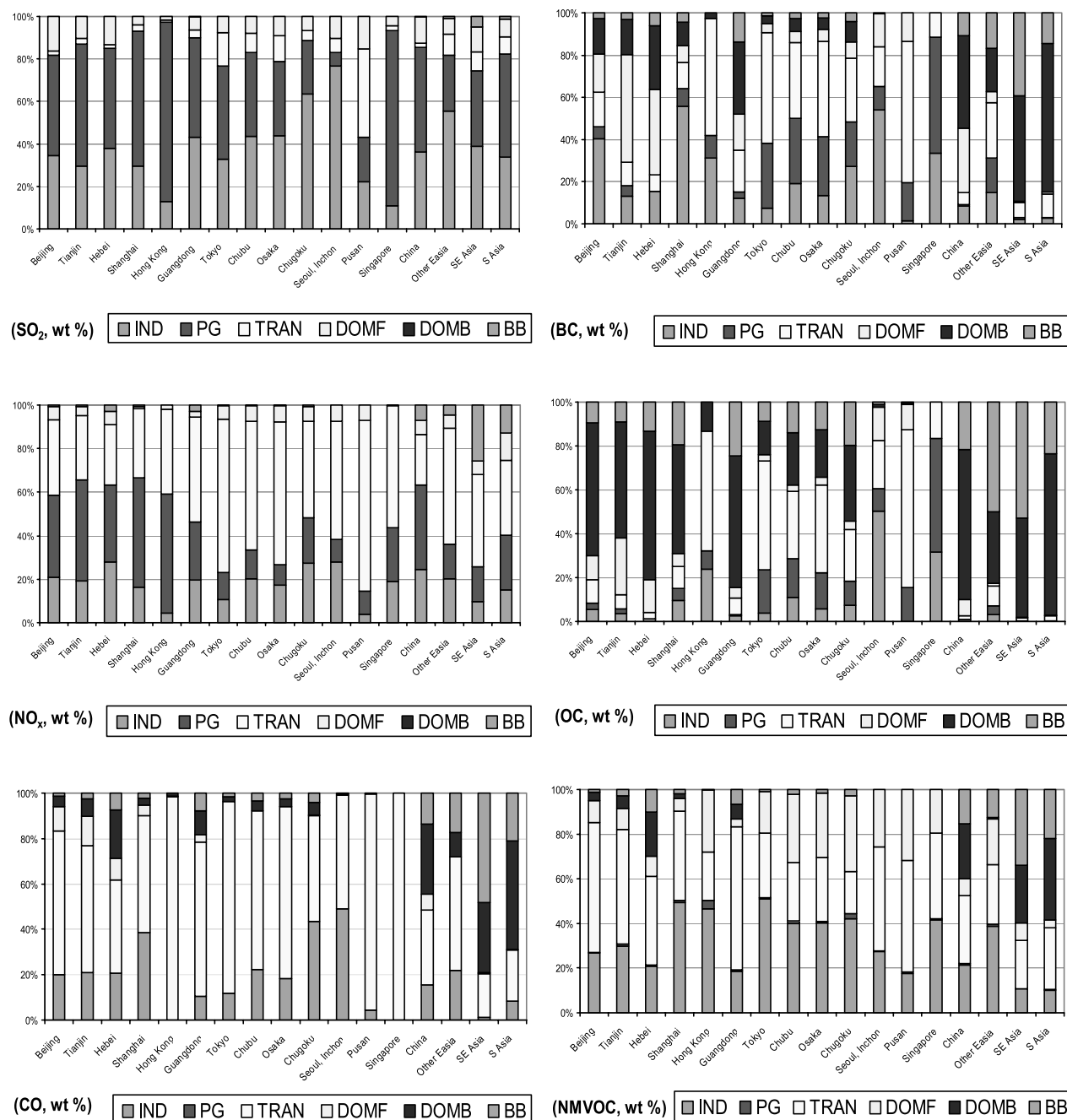
Figure 2. Contribution of various sectors to total urban and regional primary pollutant emissions in Asia in 2000: IND, industry; PG, power generation; TRAN, transportation; DOMF, domestic fossils; DOMB, domestic biofuels; BB, biomass burning. See color version of this figure at back of this issue.

in the emerging markets regions in China have a higher VOC to NO$_x$ ratios. Major anthropogenic sources of VOCs include motor vehicle exhaust, use of solvents, and the chemical and petroleum industries. NO$_x$ emission sources, mainly from the combustion of fossil fuels include motor vehicles and electricity generating stations. Because of increasing demand and advocating of low-carbon fuels, there is increasing potential for the use of natural gas in the domestic and transport sectors. Once adequate infrastructure is in place, natural gas will further change the urban emissions.

[17] Carbonaceous particles (BC and OC) account for a significant fraction of PM$_{2.5}$ in the megacities of Asia. The fractions of carbonaceous particles range from >50% in south and Southeast Asia to <50% in east Asia. The large fraction of carbonaceous particulates reflects in part the inefficient combustion of fossil fuels and biofuels in south and Southeast Asia [*Streets et al.*, 2003].

[18] The high average CO to VOC emission ratios in the cities of China (~4.7) and the Indian subcontinent (~2.8) compared to the cities in the rest of east Asia and Southeast Asia (~1.1 and ~0.9, respectively), reflect the diverse

Table 2. Primary Emission Ratios for the Cities of Asia in 2000[a]

	SO_2/NO_x	VOC/NO_x	CO/VOC	$(BC+OC)/PM_{10}$	$(BC+OC)/PM_{2.5}$
East Asia					
Beijing	2.01	1.9	5.48	0.26	0.51
Taiyuan	3.42	1.1	5.94	0.27	0.70
Tianjin	1.31	1.3	4.90	0.30	0.59
Shanghai	1.13	1.6	4.93	0.24	0.46
Qingdao	1.40	1.6	5.36	0.44	0.54
Guangzhou	1.54	1.9	3.26	0.34	0.49
Wuhan	1.67	1.0	5.14	0.43	0.55
Chongqing	4.71	2.6	5.56	0.45	0.55
Hong Kong	0.36	1.3	2.03	0.22	0.32
Seoul	0.77	0.7	0.90	0.34	0.67
Pusan	0.57	1.3	0.73	0.14	0.28
Tokyo	0.41	1.5	1.11	0.38	0.66
Osaka	0.47	1.1	1.67	0.36	0.58
Southeast Asia					
Bangkok	2.79	4.0	0.90	0.29	0.35
Singapore	0.88	0.7	1.03	0.03	0.05
Jakarta	1.46	10	1.80	0.42	0.44
Manila	4.36	5.0	0.48	0.38	0.42
Kuala Lumpur	1.13	3.1	0.65	0.25	0.37
South Asia					
Calcutta	1.06	4.1	2.71	0.27	0.34
New Delhi	1.08	2.7	3.29	0.18	0.26
Bombay	1.87	2.4	1.86	0.27	0.36
Karachi	6.20	1.6	1.18	0.24	0.32
Lahore	2.87	2.7	2.86	0.22	0.30
Dhaka	1.44	5.3	5.18	0.31	0.37

[a]Values are in kT/kT.

energy splits between coal, oil and natural gas. From Figure 3, as the cities transition their energy mix from coal intensive to oil and gas (cities on the right highly dependent on coal and those at the far left highly dependent on gas) the SO_2/NO_x and VOC/NO_x emission ratios decrease and the fraction of the carbonaceous particles in $PM_{2.5}$ increases. In addition to the large contribution to the release of local criteria pollutants, megacities also contribute significantly to greenhouse gas emissions. The growing transport sector in the Asian megacities is also the largest source of carbon dioxide (CO_2) and methane (CH_4).

3. Signatures of Megacity Plumes During Spring 2001

[19] Characterizing the role of urban plumes and their composition during the outflow conditions were important objectives of the TRACE-P and ACE-Asia experiments.
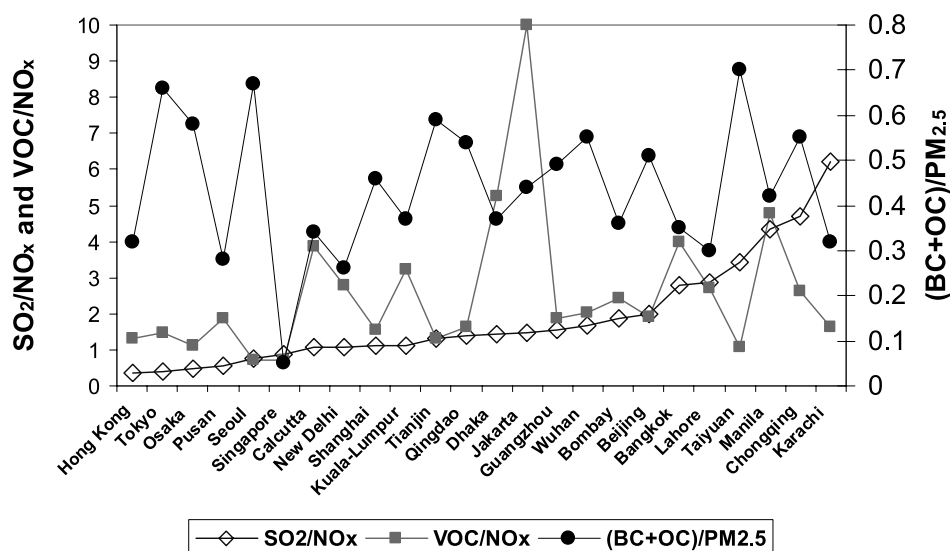

Figure 3. Primary trace gas and aerosol emission ratios (by weight) for the megacities in Asia in 2000. See color version of this figure at back of this issue.

Many experiments were conducted under strong outflow conditions downwind of megacities, and these missions often encountered fresh and aged urban pollution plumes. Measurements in these plumes provide an opportunity to study and to test the consistency of emission estimates among the fresh plumes [*Carmichael et al.*, 2003b]. One of the difficult tasks is the identification of urban plumes embedded in polluted continental outflows. To do so requires methods to identify specific plumes associated with specific cities and estimates of the age of the plumes. We used two techniques for characterizing urban signals: (1) targeted megacity simulations and (2) trajectory analysis.

[20] We performed sensitivity runs with and without megacity emissions to study the influence of megacity emissions on regional air quality and their role in the long-range transport and photochemistry in the region. For these studies we utilized the Sulfur Transport and Emissions Model 2001 (STEM-2K1) regional chemical transport model for atmospheric modeling simulations with detailed chemical mechanism (SAPRC 99) and explicit photolysis solver (NCAR Tropospheric Ultraviolet-Visible radiation model). The NORMAL simulation is our baseline run, and considers all emissions (anthropogenic and natural), deposition, gas phase chemistry, transport, diffusion, and aerosol influences on photolysis rates. This simulation is the same as the baseline simulation presented by *Carmichael et al.* [2003a] and *Tang et al.* [2003a, 2003b]. The meteorological fields were obtained using the RAMS 4.3 model in hindcast mode. The model performance and comparison of modeling results with TRACE-P and ACE-Asia measurements show good agreement with observed data, results of which are presented by *Carmichael et al.* [2003a], *Tang et al.* [2003a, 2003b], *Uno et al.* [2003a, 2003b]. The simulation with megacity emissions removed is called NOMEG. The differences between NORMAL and NOMEG simulations isolate the megacity influences.

[21] For these regional-scale simulations the model resolution was fixed at 80 × 80 km (∼1° × 1° in the midlatitudes) in rotated polar stereographic projection. The model domain presented in Figure 1 extends from eastern India and Bangladesh (74°E in longitude) in the west to Japan and Pacific Ocean (150°E in longitude) in the east and Thailand and the Philippines (10°N in latitude) in the south to Mongolia (48°N in latitude) in the north. The simulations were conducted for two months, March and April 2001, with and without megacity emissions and evaluated against the aircraft measurements obtained during the TRACE-P and ACE-Asia field experiments [*Carmichael et al.*, 2003a].

[22] Three-dimensional back trajectories were also calculated for each of the flight points at 5-min 3-min intervals for TRACE-P and ACE-Asia experiments, respectively, using the 4-dimensional modeled meteorology. Note that an individual trajectory gives only a general description of the wind field because it does not account for atmospheric processes such as vertical and horizontal mixing and diffusion or chemical evolution along the trajectory. Back trajectory analysis was used to help identify the origin of the urban plumes and to establish the air mass ages.

[23] Results for all TRACE-P and ACE-Asia flights in the western Pacific were analyzed. Illustrative examples from 2 flights are shown in Figure 4. Figure 4 presents the flight paths along with the measurements of CO, the back trajectory paths for one example segment, showing pollutant outflow conditions from one or more cities, and simulated percent contribution of megacity anthropogenic emissions to ambient mixing ratios of one pollutant averaged below 1 km during the flight period. The TRACE-P DC8 flight 13 measured concentrations of over 1000 ppbv of CO, 25 ppbv of SO_2, 10 ppbv of HCHO and 100 ppbv of O_3 along the flight track at 30°N over the Yellow Sea. Simulated megacity results indicated that in this region the Shanghai contribution was large, with the megacity contribution as high as 30% for CO and 50% for HNO_3. The observed levels of NO and nitrate indicate a fresh outflow of pollutants. Back trajectory analysis showed that the age of this plume to be less than 0.5 days. The ACE-Asia flight C130-09 measured aged pollution from Shanghai, Seoul, and Qingdao along various flight legs.

[24] The back trajectories were also used to identify individual measurements that were possibly influenced by the megacity emissions. This was achieved by keeping track of the encounters when a back trajectory passed over a megacity grid cell at an altitude <2 km. The analysis was limited to locations along the back trajectories that were within 2 km of the surface, since these are the air masses most likely to be influenced by the regional emissions. Note that all the encounters along the back trajectory were counted and that a single back trajectory could encounter more than one city (but not at the same time). Given the differences in emission ratios in each of these cities and age of these plumes, sorting data in this manner provides an opportunity to look for different megacity emission characteristics. The trajectory analysis presented here is based on meteorological data alone and a detailed analysis of the megacity points for the validation of emission data sets is presented by *Carmichael et al.* [2003b].

[25] For TRACE-P, a total of 2238 5-min merged measurement points are archived from 22 DC8 and P3 flights and for ACE-Asia, a total of 2701 3-min merged measurement points are archived from 17 C-130 flights. Figure 5 presents the statistics of the megacity encounters classified by city and estimated age of each trajectory from the source region to the point when it was intercepted by the DC8, P3 and C-130 flights. A total of 1085 points for TRACE-P and a total of 1457 points for ACE-Asia are estimated to have passed over at least one of the megacities with in a transport period of 5 days. Some import features resulting form this analysis are as follows.

[26] Because of the large number of flights along the longitude of 125°E, in the Japan Sea and Yellow Sea, a significant number of plumes were measured originating from Shanghai, Qingdao, Beijing, Taiyuan, Tianjin and Guiyang, Seoul and Pusan.

[27] The TRACE-P flights covered a relatively large area in both horizontal and vertical directions with earlier flights based out of Hong Kong and later flights out of Tokyo, Japan. This is reflected in the trajectory analysis with a spectrum of megacity signals from both northern China (Beijing, Tianjin and Taiyuan) and southern China (Guangzhou, Wuhan and Guiyang).

[28] ACE-Asia flights based out of Iwakuni, Japan flew mostly north of 30°N over the Yellow Sea at low altitudes. Their samples reflected more trajectories out of Seoul,
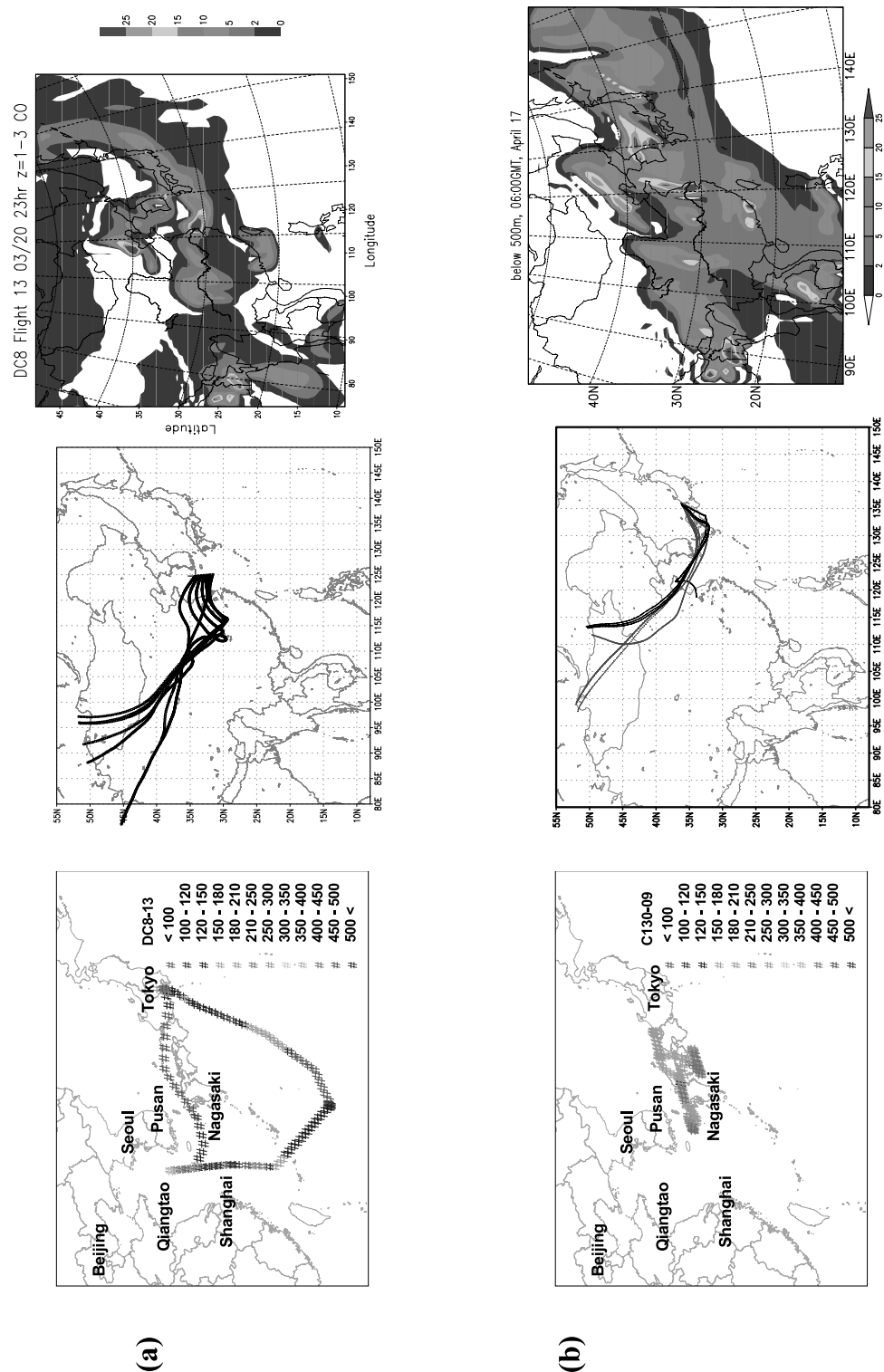
Figure 4. Identification of megacity signals using flight path with CO measurements, back trajectories, and percent contribution of megacity emissions to pollutant mixing ratios during the flight operation averaged between 0 and 500 m. (a) TRACE-P DC8-09 flight path, back trajectories between 0500 and 0530 GMT, and percent contribution to CO mixing ratios. (b) ACE-Asia C130-09 flight path with CO measurements, back trajectories between 0400 and 0500 GMT, and simulated percent contribution to CO mixing ratios. See color version of this figure at back of this issue.
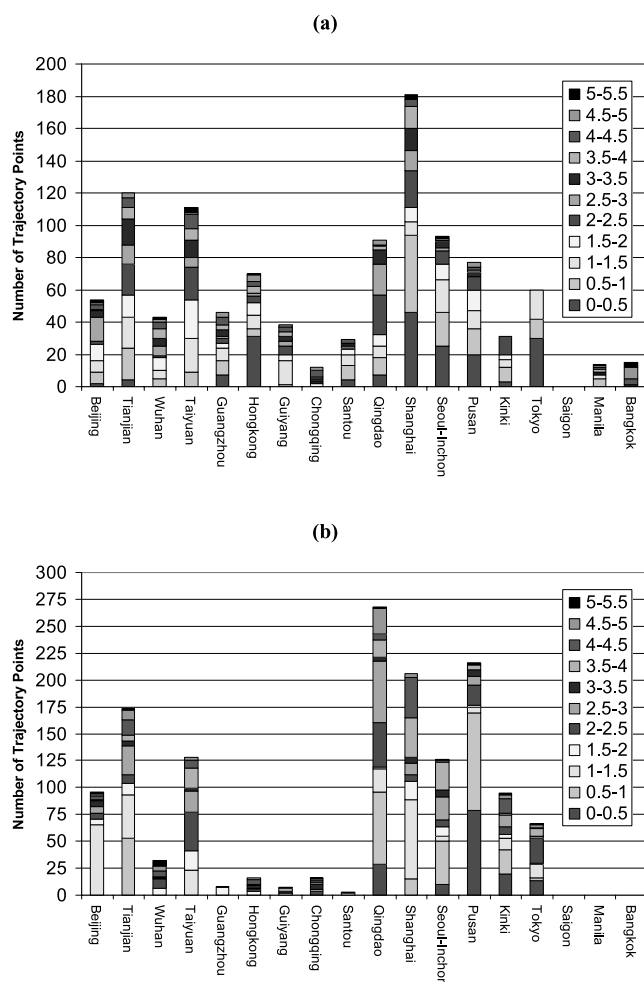
(a)

(b)

Figure 5. Statistics from backward trajectory analysis of all the measurement points along the (a) TRACE-P DC8 and P3 flight tracks and (b) ACE-Asia C-130 flight tracks. Color code indicates expected age of the trajectory from the city of origin when intercepted (in days). See color version of this figure at back of this issue.

Pusan, Qingdao, Osaka (Kinki) and Tokyo than TRACE-P measurements.

[29] Of all the cities listed, the Shanghai urban plume was intercepted the most (∼180 points) during the TRACE-P experiment, and Qingdao (∼270), Shanghai (∼210), Seoul (∼125) and Pusan (∼210) were intercepted the most during ACE-Asia. The ages of the air masses were estimated to range from less than 0.5 to 5 days.

[30] Approximately 35 points from TRACE-P and ACE-Asia had back trajectories reaching Chongqing with trajectory ages ranging from 2–5 days.

[31] Hong Kong and Tokyo plumes with ages of less than 0.5 days were obtained during takeoff and landing periods.

[32] The data classified by specific megacity influence was then used to help identify air mass signatures. Results for the DC-8 and P-3 data for the cities of Tokyo, Shanghai, Hong Kong and Qingdao are shown in Tables 3 and 4, respectively. Shown are the observed regression slopes and correlation coefficients for selected species when regressed against observed CO, acetelyne and benzene. The tracers

were chosen on the basis of the previous analysis of *Blake et al.* [2003]. For example, halon 1211 (CF_2ClBr) is a fire retardant still produced in China, and the slopes for this species are elevated in Chinese cities. CH_3Cl is a tracer for biomass and biofuel and these ratios are also elevated in Chinese cities, as are the ratios involving CCl_4 and OCS. In contrast HCFC-141b is enhanced in Japanese cities, as are the ratios involving CH_3Br.

[33] The identification of megacity-influenced points also allows for additional analysis to evaluate the emissions inventory utilized in the study. The ratios of species often can provide insights into emission characteristics, and comparison of observed ratios with emission ratios provides an important consistency test. Data points of air masses younger than 1 day, which reflect the strongest emission signatures and the least uncertainty, were used for such an analysis. A detailed discussion of how the regression analysis of predicted values were compared with the observation-based ratios is presented by *Carmichael et al.* [2003b]. Here we focus on the observation-based ratios and their comparison with the emission estimates. A summary of the regression ratios and emission-based ratios are presented in Table 5. A direct comparison of observation-based with emission-based ratios as a check on consistency of the emissions is limited to those species that have similar lifetimes in the atmosphere. Of the species shown in Table 5, C_2H_6/CO and BC/CO fit this requirement. For these species there is general consistency between the observed ratios and the emissions. Take as an example the BC/CO ratios. The observations show that Tokyo has the largest value, followed by Seoul, and then by the Chinese cites (all with very similar values). These ratios are consistent with the emissions ratios, but the value for Seoul, while larger than that for the Chinese cities, is lower than expected from the emissions. This difference between the observed ratio and the emissions reflects the fewer number of points available for the Seoul plume and the large impact of the nearby China emissions (with a lower ratio).

[34] The observed regional differences in the ratios for the various cities are anticipated by the variation in the sectoral contributions to emissions for these cities as shown in Figure 2. For example, on the basis of the emission estimates, the SO_x to CO ratios are higher in the Chinese megacities, such as Beijing and Qingdao, compared to Seoul and Tokyo, because of higher coal consumption levels. These features are found in the observation-based ratios. Furthermore, the higher NO_y and SO_x ratios observed for Seoul, Tokyo and Pusan compared to Beijing and Qingdao, are consistent with the city-specific emission ratios. It should be noted that the negative slopes for the ratios involving SO_x around Tokyo are primarily due to the large impact of volcanic emissions. Within the Chinese cities, often the north-central China cities of Tianjin, Beijing, and Qingdao were found to have observation-based ratios that are very similar to each other, but which are different than those for Shanghai (see, for example, NO_y/CO and SO_x/CO).

[35] These findings regarding the regional characteristics of the Asian megacities are also supported through cluster analysis performed using the observed ratios. Cluster analysis is a data analysis tool that identifies structures in the data. We applied this method to see whether megacities in

Table 3. Trace-P DC8 Flights Megacity Analysis for Tokyo, Shanghai, Hong Kong, and Qingdao Based on Backward Trajectory[a]

	Tokyo		Shanghai		Hong Kong		Qingdao	
Species	Slope	R^2	Slope	R^2	Slope	R^2	Slope	R^2
CF_2ClBr/CO	1×10^{-6}	0.66	0.00001	0.45	0.00006	0.93	NA	NA
CF_2ClBr/C_2H_4	0.00006	0.58	0.0017	0.62	0.01	0.98	NA	NA
$CF_2ClBr/benzene$	0.00024	0.65	0.0025	0.48	0.028	0.94	NA	NA
CH_3CCl_3/CO	0.00003	0.95	0.00002	0.34	0.0001	0.82	NA	NA
CH_3CCl_3/C_2H_4	0.0003	0.99	0.002	0.52	0.025	0.99	NA	NA
$CH_3CCl_3/benzene$	0.01	0.93	0.0034	0.36	0.07	0.99	NA	NA
C_2Cl_4/CO	0.0004	0.96	0.00004	0.9	0.0003	0.84	NA	NA
C_2Cl_4/C_2H_4	0.03	0.92	0.009	0.91	0.054	0.99	NA	NA
$C_2Cl_4/benzene$	0.12	0.99	0.015	0.94	0.15	0.99	NA	NA
CH_3Br/CO	0.0004	094	0.00002	0.94	0.15	0.99	NA	NA
CH_3Br/C_2H_4	0.03	0.88	0.003	0.84	0.003	0.92	NA	NA
$CH_3Br/benzene$	0.12	0.98	0.0044	0.69	0.0085	0.97	NA	NA
$HCFC-141b/CO$	0.0004	0.9	0.00002	0.24	0.00004	0.81	NA	NA
$HCFC-141b/C_2H_4$	0.03	0.97	0.001	0.42	0.0067	0.99	NA	NA
$HCFC-141b/benzene$	0.12	0.86	0.0018	0.25	0.02	0.99	NA	NA
$HCFC-22/CO$	0.0008	0.98	0.0001	0.5	0.0003	0.76	NA	NA
$HCFC-22/C_2H_4$	0.07	0.98	0.017	0.62	0.056	0.96	NA	NA
$HCFC-22/benzene$	0.27	0.98	0.026	0.51	0.16	0.99	NA	NA
CCl_4/CO	0.00003	0.92	0.00006	0.5	0.00005	0.6	NA	NA
CCl_4/C_2H_4	0.002	0.86	0.01	0.78	0.006	0.73	NA	NA
$CCl_4/benzene$	0.0084	0.96	0.014	0.63	0.018	0.82	NA	NA
CH_3Cl/CO	0.0006	0.95	0.0016	0.75	0.0003	0.82	NA	NA
CH_3Cl/C_2H_4	0.05	0.94	0.35	0.95	0.03	0.49	NA	NA
$CH_3Cl/benzene$	0.2	0.96	0.56	0.85	0.078	0.39	NA	NA
OCS/CO	0.0006	0.99	0.0001	0.92	0.0007	0.84	NA	NA
OCS/C_2H_4	0.06	0.97	0.2	0.69	0.12	0.99	NA	NA
$OCS/benzene$	0.2	0.97	0.39	0.9	0.35	0.94	NA	NA
$CFC-11/CO$	0.00015	0.87	0.00004	0.64	0.0001	0.47	NA	NA
$CFC-11/C_2H_4$	0.01	0.95	0.0075	0.69	0.013	0.81	NA	NA
$CFC-11/benzene$	0.04	0.81	0.013	0.68	0.038	0.88	NA	NA
$CFC-12/CO$	0.0001	0.92	0.00007	0.4	0.0002	0.61	NA	NA
$CFC-12/C_2H_4$	0.01	0.9	0.0065	0.28	0.03	0.91	NA	NA
$CFC-12/benzene$	0.04	0.95	0.013	0.4	0.093	0.96	NA	NA

[a]Units are in ppbv/ppbv. NA indicates that the number of data points was not sufficient to produce a statistically significant slope.

Asia can be grouped or distinguished using the observed ratios. A similar analysis by *Woo et al.* [2003] found that regional emissions in Asia could be characterized by ~10 characteristic emission groupings. The ratios used in the megacity analysis were C_2H_6/CO, C_2H_2/CO, C_3H_8/CO, NO_y/CO, SO_x/CO, NO_y/SO_x, C_2H_6/C_2H_2, C_2H_6/C_3H_8, C_2H_6/C_2H_4, C_2H_6/C_3H_6, SO_x/C_3H_6, and SO_x/C_2H_2, and the results are shown in Figure 6. The component plot shows the location of each megacity in terms of two principal components axis that were derived from the cluster analysis of the chemical species ratios. As shown, the analysis clusters megacities in Japan (Tokyo as tok_ob), Korea (Seoul and Pusan, as sel_ob and pus_ob, respectively), and China (Beijing, Tianjin, Qingdao, and Shanghai, as bei_ob, tij_ob, qid_ob, and sha_ob, respectively), with Hong Kong (as hok_ob) separate by itself from the other Chinese cities. Combining these results with the emissions information we find cities with (1) high coal use (Chinese cities except Hong Kong), (2) high oil/gas use (Korean cities), (3) high oil/gas use plus biomass burning plume (Hong Kong), and (4) high oil/gas use plus volcano (Tokyo).

[36] Outside of the C_2H_6/CO and BC/CO values, the other observation-based ratios shown in Table 5 differ in magnitude significantly from the emissions ratios, as expected. For example, the observation-based NO_y/CO values are 5–10 times smaller than the emission values.

This reflects the fact that the lifetime of NO_y in the springtime in east Asia is ~1/5 that of CO [*Koike et al.*, 2003]. In addition the observation-based NO_y/SO_x values are lower than the emissions. This reflects the fact that the lifetime of NO_y is lower than that for SO_x. Thus this ratio decreases with air mass age. Below we look at ratios involving formaldehyde to illustrate how the ratios of species can differ from their emissions.

[37] HCHO is important as it is both directly emitted in the megacities and produced by oxidation of hydrocarbons in the megacity plumes. In addition via photolysis and reaction with OH it constitutes a major source of ambient CO. When the observational data are stratified into megacity and other categories, it is found that the HCHO/CO ratio (ppbv/ppbv) for the megacities is 0.007 compared to 0.002 for the other data points. The HCHO/CO ratios are on average higher than those observed in INDOEX. The HCHO/CO ratios in the emissions inventory vary from 0.009 for Hong Kong to 0.002 in Shanghai.

[38] The number of data points associated with individual megacities allows for an investigation of this ratio with age of the air masses. For fresh urban plumes with a back trajectory age of less than a day from a megacity, ratios as high as 0.012 ppbv HCHO to ppbv CO are found, decreasing to values below 0.005 for plumes with ages of 5 days. For Shanghai, the HCHO/CO value for plumes less than 1 day of age based on the aircraft measurements is 0.01,

Table 4. Trace-P P3 Flights Megacity Analysis for Tokyo, Shanghai, Hong Kong, and Qingdao Based on Backward Trajectory[a]

	Tokyo		Shanghai		Hong Kong		Qingdao	
Species	Slope	R^2	Slope	R^2	Slope	R^2	Slope	R^2
CF_2ClBr/CO	2×10^{-6}	0.29	8×10^{-6b}	0.96	NA	NA	3×10^{-6}	0.44
CF_2ClBr/C_2H_4	0.00006	0.09	0.002^b	0.53	NA	NA	0.0017	0.77
$CF_2ClBr/benzene$	0.0005	0.37	0.0035^b	0.72	NA	NA	0.0013	0.73
CH_3CCl_3/CO	0.00006	0.51	0.00001	0.79	NA	NA	0.00005	0.15
CH_3CCl_3/C_2H_4	0.0086	0.95	0.002^b	0.45	NA	NA	0.018	0.87
$CH_3CCl_3/benzene$	0.028	0.73	0.005^b	0.57	NA	NA	0.01	0.48
C_2Cl_4/CO	0.0005	0.67	0.00007	0.36	NA	NA	0.0002	0.09
C_2Cl_4/C_2H_4	0.076	0.99	0.01^b	0.57	NA	NA	0.046	0.61
$C_2Cl_4/benzene$	0.24	0.78	0.016^b	0.54	NA	NA	0.024	0.28
CH_3Br/CO	0.0001	0.6	0.00002^b	0.66	NA	NA	0.00006	0.04
CH_3Br/C_2H_4	0.009	0.29	0.0025^b	0.35	NA	NA	0.004	0.12
$CH_3Br/benzene$	0.03	0.26	0.005^b	0.53	NA	NA	0.002	0.05
$HCFC-141b/CO$	0.0004	0.57	0.0002^b	0.004	NA	NA	0.00004	0.04
$HCFC-141b/C_2H_4$	0.06	0.98	0.001^b	0.03	NA	NA	0.005	0.38
$HCFC-141b/benzene$	0.19	0.74	0.0008	0.007	NA	NA	0.003	0.14
$HCFC-22/CO$	0.0008	0.65	0.0002	0.22	NA	NA	0.0002	0.10
$HCFC-22/C_2H_4$	0.12	0.99	0.0077	0.06	NA	NA	0.065	0.74
$HCFC-22/benzene$	0.41	0.79	0.015	0.1	NA	NA	0.035	0.35
CCl_4/CO	0.00002	0.52	0.00004^b	0.94	NA	NA	0.00004	0.17
CCl_4/C_2H_4	0.002	0.65	0.01^b	0.65	NA	NA	0.015	0.81
$CCl_4/benzene$	0.007	0.51	0.02	0.9	NA	NA	0.009	0.44
CH_3Cl/CO	0.0003	0.8	0.0012^b	0.98	NA	NA	0.0004	0.47
CH_3Cl/C_2H_4	0.04	0.54	0.47^b	0.79	NA	NA	0.24	0.78
$CH_3Cl/benzene$	0.16	0.62	0.86	0.94	NA	NA	0.18	0.70
OCS/CO	0.0006	0.52	0.0008	0.94	NA	NA	0.001	0.9
OCS/C_2H_4	0.02	0.06	0.14	0.37	NA	NA	0.31	0.11
$OCS/benzene$	0.17	0.36	0.32^b	0.66	NA	NA	0.59	0.61
$CFC-11/CO$	0.00009	0.72	0.00003^b	0.67	NA	NA	0.00007	0.13
$CFC-11/C_2H_4$	0.014	0.93	0.0077^b	0.59	NA	NA	0.021	0.63
$CFC-11/benzene$	0.051	0.86	0.014^b	0.73	NA	NA	0.012	0.35
$CFC-12/CO$	0.00014	0.66	0.00005^b	0.59	NA	NA	0.0006	0.003
$CFC-12/C_2H_4$	0.02	0.87	0.018	0.83	NA	NA	0.018	0.36
$CFC-12/benzene$	0.08	0.87	0.03	0.81	NA	NA	0.007	0.09

[a]Units are in ppbv/ppbv. NA indicates that the number of data points was not sufficient to produce a statistically significant slope.
[b]Slopes from the DC-8 data and P-3 data agree within ~30%.

Table 5. Observation-Based and Emission-Based Ratios of Selected Species for the Megacities of Asia During the TRACE-P Experiment[a]

Species	C_2H_6/CO	C_3H_8/CO	BC/CO	NO_y/CO	SO_x/CO	C_2H_2/CO	NO_y/SO_x
Seoul							
Observation	0.007	0.007	0.014	0.003	0.008	0.004	0.76
Emission	0.009	0.010	0.030	0.420	0.210	0.008	2.00
Pusan							
Observation	0.007	0.004		0.016	0.012	0.004	0.83
Emission	0.003	0.003	0.010	0.190	0.060	0.003	3.00
Tokyo							
Observation	0.004	0.007	0.017	0.04	−0.012	0.004	−0.18
Emission	0.005	0.005	0.020	0.210	0.040	0.003	5.30
Shanghai							
Observation	0.004	0.003	0.011	0.011	0.028	0.008	0.35
Emission	0.004	0.005	0.010	0.110	0.110	0.006	1.00
Hong Kong							
Observation	0.005	0.002	0.011	0.001	0.003	0.005	0.2
Emission	0.012	0.011	0.010	0.720	0.270	0.007	2.7
Tianjian							
Observation	0.004	0.002	0.011	0.013	0.032	0.002	0.43
Emission	0.005	0.006	0.010	0.100	0.110	0.006	0.90
Beijing							
Observation	0.005	0.002		0.018	0.037	0.002	0.46
Emission	0.004	0.005	0.010	0.05	0.060	0.007	0.90
Qingdao							
Observation	0.004	0.002	0.011	0.015	0.035	0.002	0.45
Emission	0.005	0.006	0.010	0.110	0.200	0.009	0.60

[a]The measurement points have an air mass of less than 1 day from the megacity to the point of intersection along the flight segment.

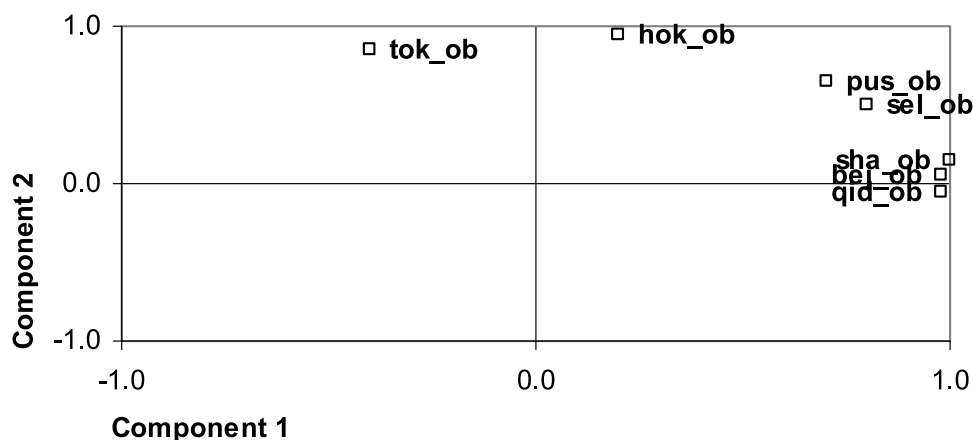## Component Plot in Rotated Space

Figure 6. Principal component analysis of Asian megacities using observation-based ratios: bej, Beijing; tij, Tianjin; qid, Qingdao; sha, Shanghai; hok, Hong Kong; sel, Seoul-Inchon; pus, Pusan; tok, Tokyo.

while the emissions ratio is 0.002. So it is interesting to investigate how the HCHO to CO ratios vary as air masses move away from the urban areas. Plotted in Figure 7 are the observed HCHO to CO ratios versus the age of the air mass for the points identified as being associated with Shanghai plumes. This analysis shows that the HCHO/CO starts at a value near that of the primary emissions, then rapidly increases, reaching a maximum of 0.018 in air masses of ~0.5 days, then decreases to a minimum value at ~1 days, and then increases and levels off at a value of ~0.003 to 0.004 (after 3–4 days). The model results are also shown, and the model is able to capture this behavior, although it is not able to resolve the magnitude of the peak value.

[39] To better understand the processes contributing to this behavior an analysis was performed of air parcels released from Shanghai. Along forward trajectories originating from Shanghai the chemical production and destruc-

tion of HCHO was calculated using results from the 3-D model and a full-chemistry point model. This point model employed the same chemical mechanism as the 3-D model but it ran only in situ assuming quasi-equilibrium conditions and utilized as inputs the initial conditions from the 3-D model along the trajectory paths. Since the output of the 3-D model was interpolated spatially and temporally, the calculation was performed for 10 min intervals so that convergence of the concentration of short-lived species was completed. An example is shown in Figure 8 for a parcel released from Shanghai at 0000 GMT on Julian day 76 (17 March 2001). The trajectory path is shown, along with the HCHO/CO evolution with time along the trajectory. The behavior in time is qualitatively similar to that shown in Figure 7. The fact that the 3-D model and the box model produce nearly identical results (see middle panel) shows that the HCHO levels are governed by the photochemistry. The HCHO/CO ratio reached its highest value during
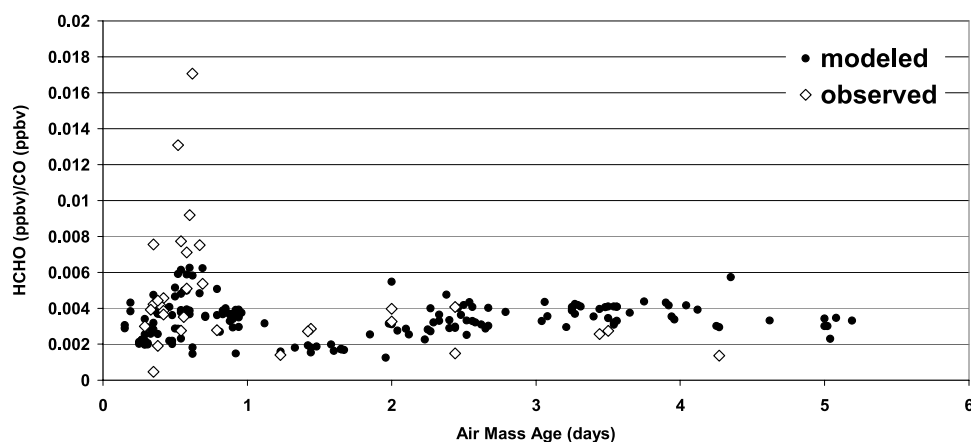

Figure 7. Observed HCHO/CO values in Shanghai plumes as a function of air mass age. Modeled values for the same data points are also shown.
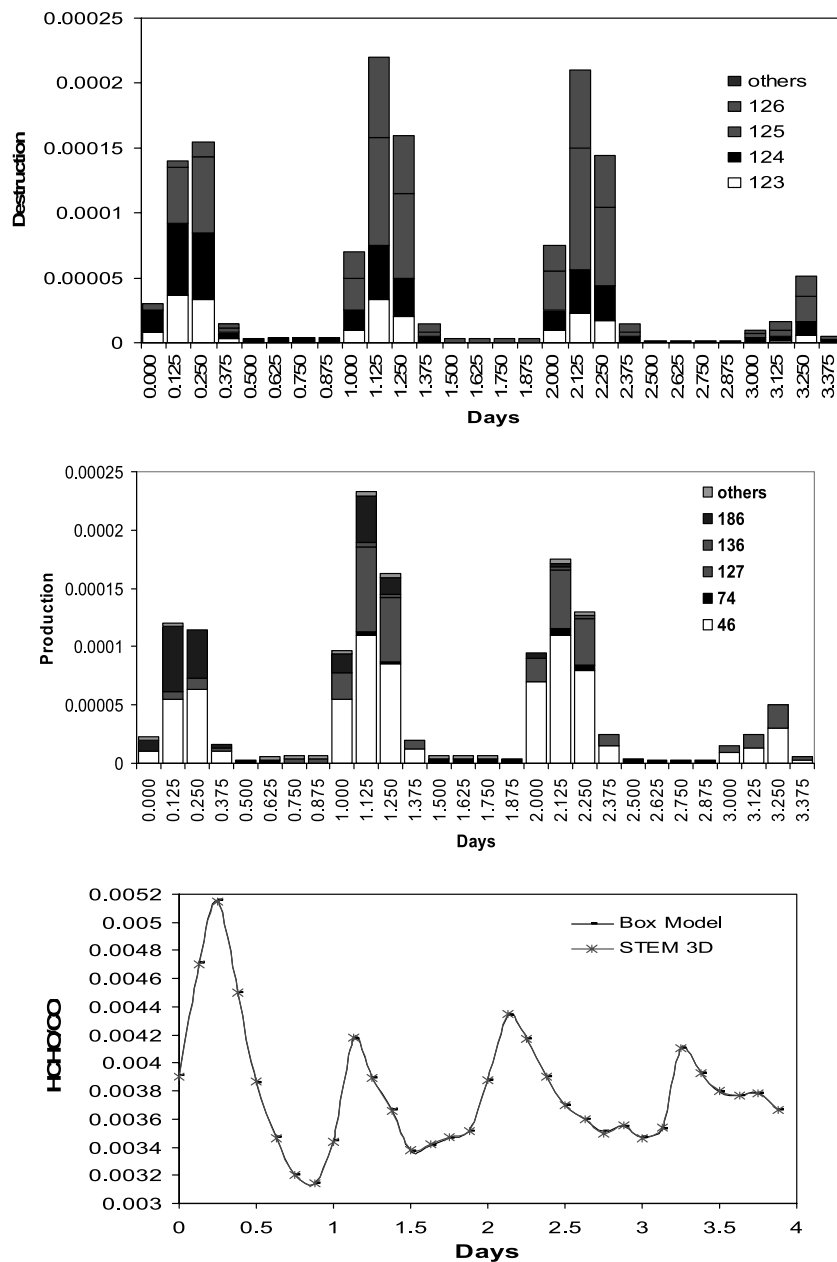
Figure 8

daytime, which reflects the importance of VOC oxidization by OH. This result also illustrates that HCHO signals sampled downwind of Shanghai are not due solely to the HCHO emission, but rather are heavily influenced by the emitted VOC and subsequent oxidization. To help quantify the causes of the changes in HCHO/CO, the details of the chemical production and destruction processes were calculated. The rapid increase in HCHO/CO at early times is associated with ethene and ethane oxidation pathways. At later times as ethene was depleted, HCHO is produced through the methane oxidation initiated pathway. Also the integrated contribution of acetone and MEK increases with time (by an order of magnitude). These results illustrate how the emissions used in the analysis, along with the model, can provide insights into the evolution of ratios of reactive species.

[40] One method to quantify the comparison of ratios of species with different lifetimes with respect to the emission-based estimates is to compare the observation-based ratios with model-based values. The model-based ratios are calculated from the emission inventory, taking into account the effects of subsequent chemistry and removal on the species ratios. A consistency between the observation-based and model-based values, infers consistency of the emissions. A discussion of model-based values in comparison with the observations is presented by *Carmichael et al.* [2003b].

4. Ambient Chemical "Footprints" of Asian Megacities

[41] As discussed above megacity plumes of various ages were sampled frequently during the ACE-Asia and TRACE-P experiments. However, we are also interested in assessing the impact of the emissions from these cities on a longer-term basis. Here we characterize the March–April mean contributions of megacity emissions to ambient pollutant distributions. Monthly averaged mixing ratios with all the emission sources included, along with the percentage contribution due to megacity emissions (defined as ((NORMAL-NOMEG)/NORMAL)*100) for O_3, CO, SO_2, H_2SO_4, HCHO, and NO_z (i.e., $NO_y - NO_x$) below 1 km are presented in Figure 9. To aid in the discussion we also define a megacity footprint of a specific species to be the area where the megacity emissions contribute to 10% or higher of the monthly mean ambient concentrations. The 10% value was chosen to define roughly the area where the megacities have a disproportional role on ambient levels (as the megacity emissions account for ∼10% of the anthropogenic emissions in Asia).

[42] Below 1 km, for SO_2, H_2SO_4, HCHO, and NO_z, the contribution of megacity emissions to ambient levels exceeds 30% for regions extending hundreds of kilo-

meters from the urban centers. The megacity footprint of sulfate is larger than that for SO_2 and covers ∼25% of the modeling domain. Please note the large SO_2 concentrations east of Tokyo for the all sources case. This reflects the large emissions from the Miyakejima volcano that occurred during the experimental period (estimated to be ∼100 times larger than the Tokyo city SO_2 emissions).

[43] The region with the largest influence from the megacity emissions is the Sea of Bengal. Because of strong monsoon winds during the springtime, most of the emissions from Bangkok, Dhaka, and Calcutta find their way into the marine boundary layer of the Sea of Bengal. In this region the megacity influence for many species exceed 20% and are often above 50%.

[44] NO_z is an indicator for photochemical activity and is usually correlated with O_3 in the areas downwind of source regions [*Trainer et al.*, 1993]. Megacity contributions of over 30% are shown around Beijing, Seoul and Tokyo and over 10% over the western Pacific Ocean. The large megacity contribution to HNO_3 mixing ratios (not presented in Figure 9) around the cities of Hong Kong, Guangzhou, Chongqing, Shanghai, Korean peninsula, and northern Japan reflect significant influence of NO_x emissions from mobile sources.

[45] The megacity footprint for CO is smaller than that for other primary species, reflecting the fact that CO sources in Asia are more diverse, with a large contribution from non-urban sources (e.g., small cottage industries in rural areas, biomass and biofuels burning, and biogenic oxidation) [*Tang et al.*, 2003a, 2003b; *Woo et al.*, 2003]. Within the vicinity of the cities, the contributions are as high as ∼15% in Beijing, Seoul, Shanghai, and Calcutta and average ∼4% over the rest of east Asia, the western Pacific Ocean and the Yellow Sea region. Individual megacity plumes sampled during the field experiments do show strong CO signals (as discussed in section 4).

[46] For O_3, megacity emissions contributions from 2% to 10% are predicted over the western Pacific, southeast China, and northern Indian Ocean. Negative values are calculated around the cities of Shanghai, Beijing, Seoul, Pusan, and Tokyo. This behavior reflects the low VOC/NO_x ratios and VOC limitation in these cities as discussed by *Carmichael et al.* [2003a]. The highest ozone concentrations associated with pollutants emitted from megacities are located over the East China Sea.

[47] The megacity footprint for formaldehyde is larger than that for ozone. As discussed previously, HCHO is both directly emitted in the megacities and formed in the megacity plumes. As a result the megacity footprint extends over the western Pacific Ocean, the Yellow Sea and the Sea of Bengal. Because of the strong outflow conditions in the spring time, significant amounts of slow

Figure 8. Calculated HCHO/CO along the path of a forward trajectory originating from Shanghai on 17 March (Julian day 76) at 0100 GMT. Destruction and production pathways are also shown. The related reactions are (46) $C\_O_2 + NO \rightarrow NO_2 + HCHO + HO_2$, (74) $CCO\_O_2 + C\_O_2 \rightarrow CH_3COOH + HCHO$, (123) $HCHO + hv \rightarrow 2HO_2 + CO$, (124) $HCHO + hv \rightarrow CO$, (125) $HCHO + OH \rightarrow HO_2 + CO$, (126) $HCHO + HO_2 \rightarrow HOCOO$, (127) $HOCOO \rightarrow HO_2 + HCHO$, (136) $ACETONE + OH \rightarrow HCHO + CCO\_O_2 + R_2O_2$, and (186) $ETHENE + OH \rightarrow RO_2\_R + 1.61HCHO + 0.195CH_3CHO$. Here C_O_2 represents methyl peroxy radicals; CCO_O_2 represents acetyl peroxy radicals; HOCOO is the radical formed when HCHO reacts with HO_2; and RO_2_R and R_2O_2 are the peroxy radical operators representing NO to NO_2 conversion with and without HO_2 formation, respectively. See color version of this figure at back of this issue.
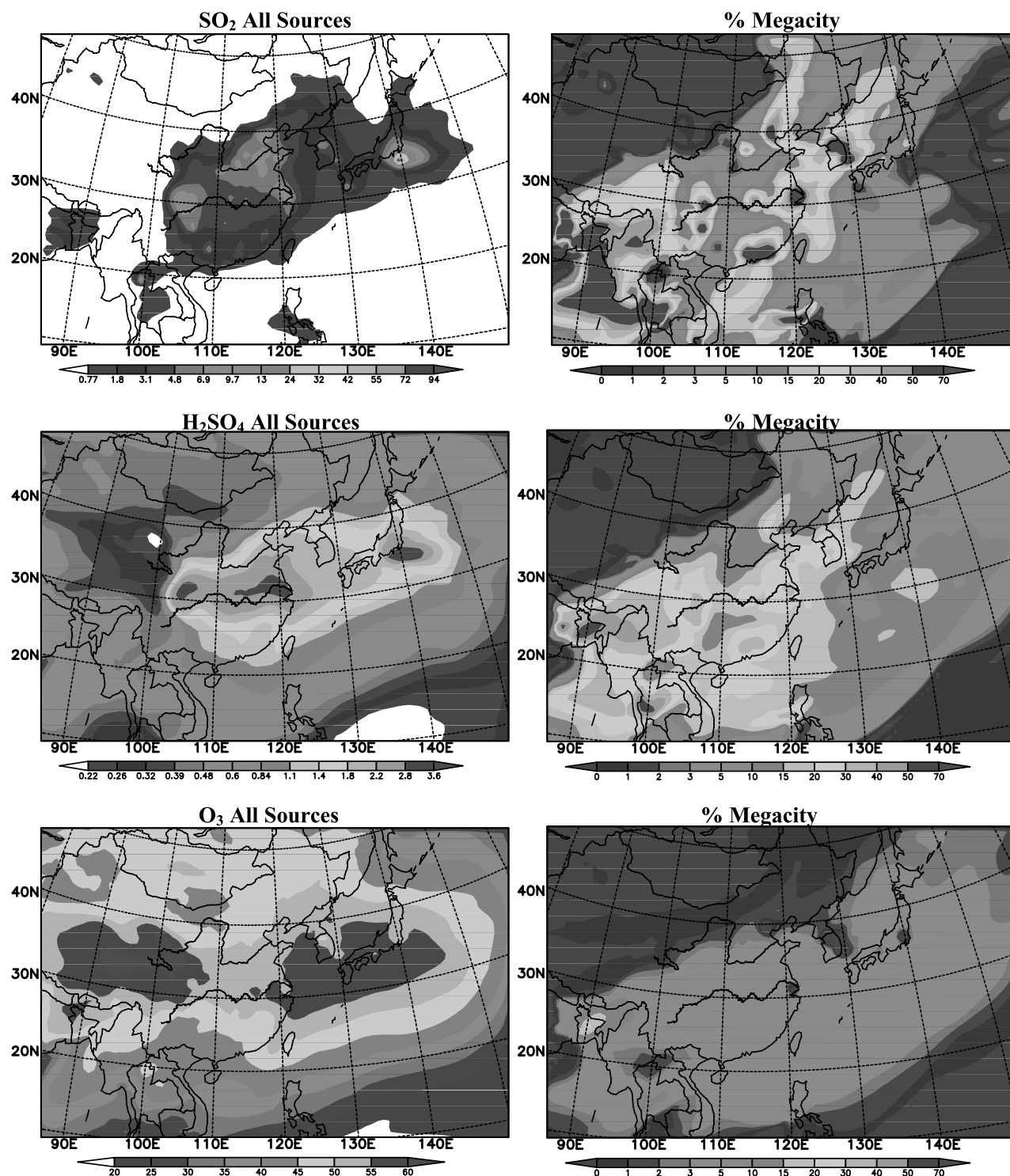
Figure 9. Simulated monthly average mixing ratios (ppbv) with all the anthropogenic and biomass sources included and percentage contribution of Asian megacity emissions averaged below 1 km during the period of March 2001. See color version of this figure at back of this issue.

reacting VOCs emitted from the megacities (not presented in Figure 9) are observed over a wide area of western Pacific Ocean. These hydrocarbons contribute to HCHO production and thus enhance the downwind extent of the HCHO megacity footprint.

[48] The influence of the megacities extends above the mixing layer. For example, the megacity footprint at 3 km

encompass broad areas downwind of Beijing, Calcutta, Chongqing and Hong Kong.

5. Discussion

[49] As discussed above the contribution of megacity emissions to the ambient levels of O_3 in Asia can be
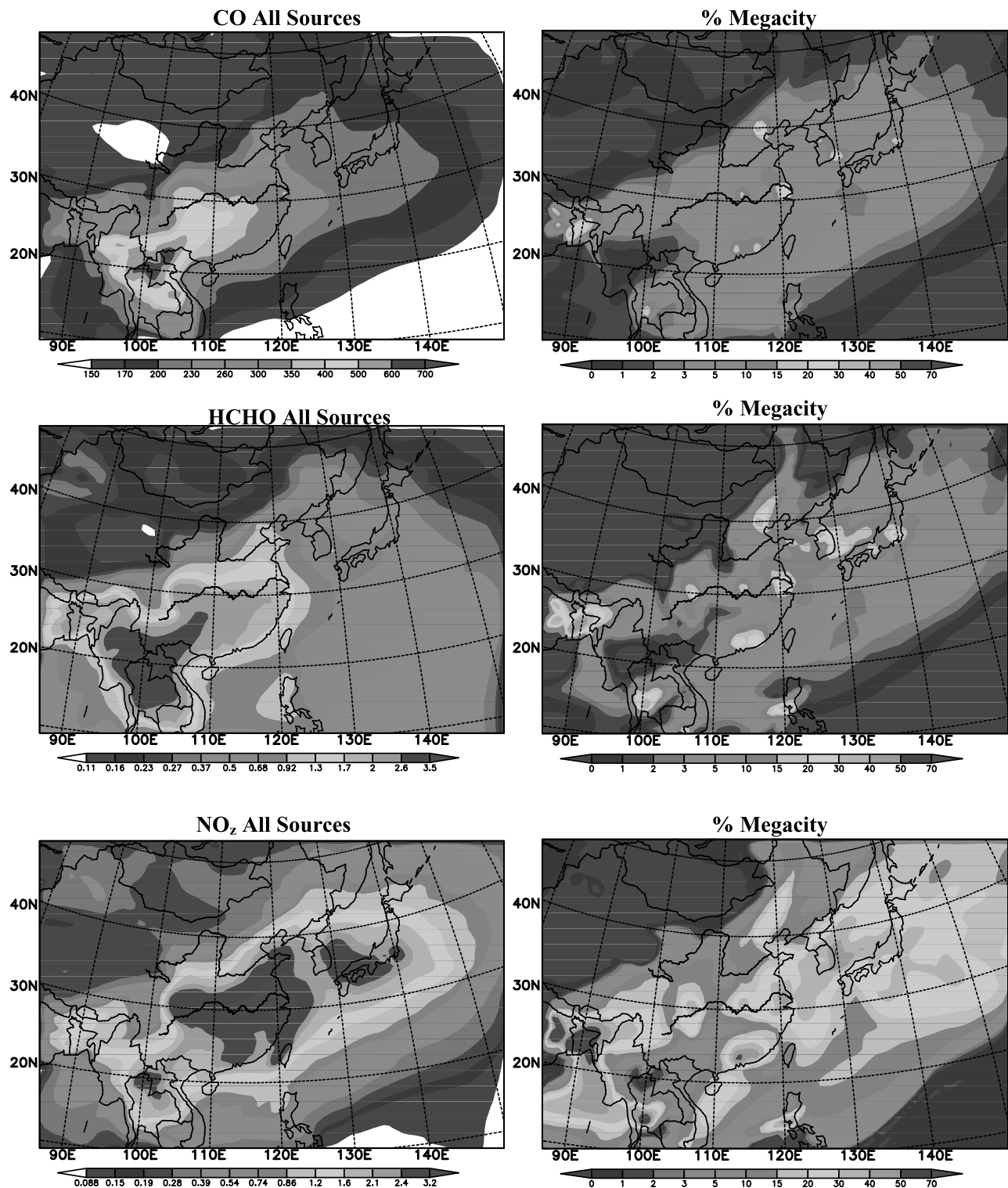
Figure 9. (continued)

significant, with percentages of up to 20% in the marine boundary and in specific plumes. However, when taken on average the megacity contribution is typically less than 5% (as shown in Figure 9) for the spring periods studied in this paper. Because of the changing emission trends in Asia, the chemical conversion regimes may change in the future. Figure 10 illustrates the role of NO_x and VOC emissions

(primary emissions that are expected to change dramatically in the future because of rapid motorization in the developing country cities) from megacities on O_3 production in Asia. Three sets of runs were conducted, the first two with the doubling of the NO_x and VOC emissions, respectively.

[50] Shown are percentage changes in O_3 mixing ratios from the base case with all the emissions included, and the
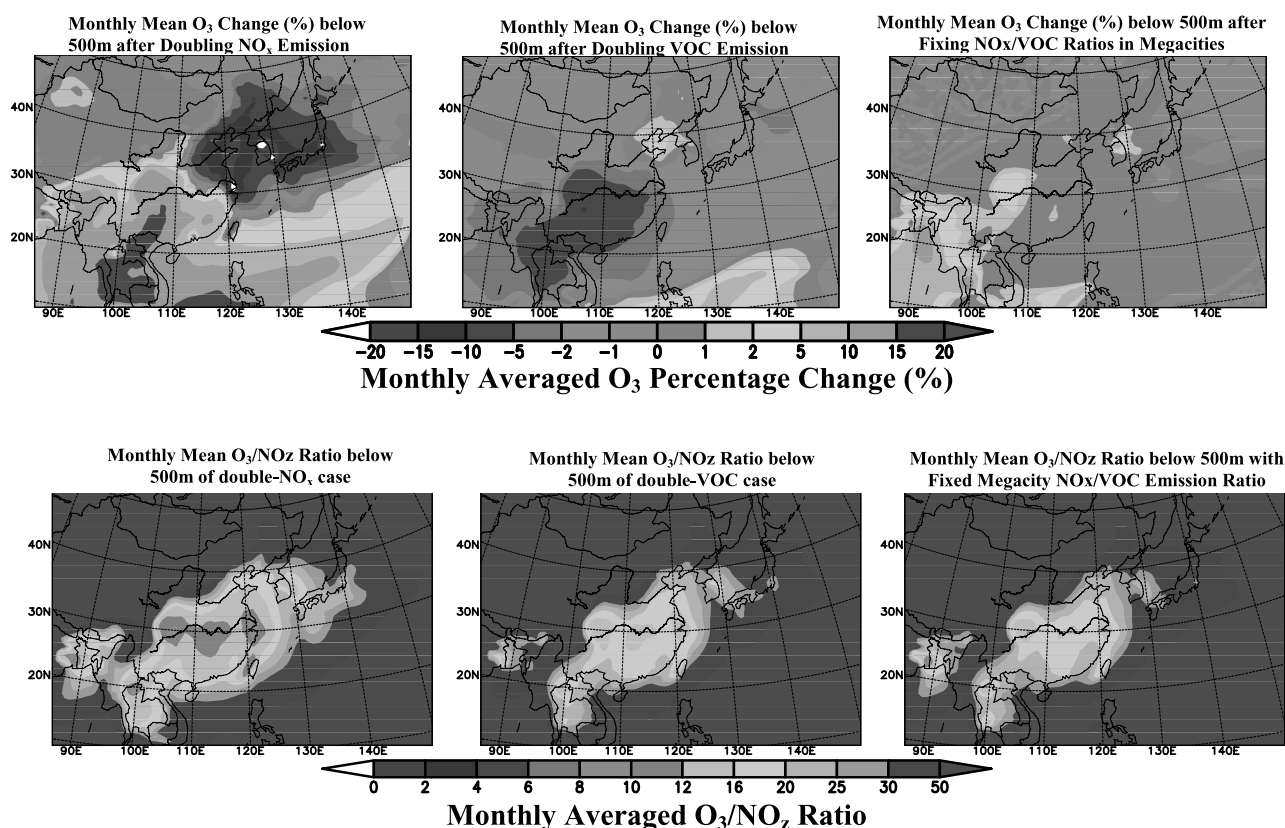
Figure 10. Percentage change in monthly average O_3 concentrations and ratio of monthly average O_3 to NO_z mixing ratios upon doubling of NO_x and VOC emissions below 500 m. See color version of this figure at back of this issue.

ratio of monthly average O_3 and NO_z mixing ratios for the NO_x and VOC cases. In the increased NO_x simulation ($2xNO_x$ case), much of the emitted NO_x is titrated with locally produced O_3 and OH, resulting in reductions in O_3 of over 20% around Seoul, Shanghai, Tokyo, Beijing, Taiyuan, and Tianjin and much of the highly industrialized northeast Asia. In high-VOC/NO_x regions of Southeast Asia and over the Indian subcontinent, increases in NO_x emissions enhance O_3 levels by as much as 25%. Also, the O_3/NO_z ratios suggest that a much larger portion of east Asia becomes VOC sensitive compared to the present conditions. The higher VOC to NO_x ratios lead to enhanced OH, HCHO and CO levels and in turn higher O_3 levels ($\sim$5% around Beijing and Seoul).

[51] These first two emission scenarios represent sensitivity studies and do not reflect likely emission trajectories. More plausible scenarios can be guided by the megacity emission information shown in Figure 3. As discussed in section 2 the emission ratios reflect in large part cities at different locations on the development curve. For example, the growth in road transport is unlikely to be curbed in the developing countries any time soon. Economic activity in these countries is highly dependent on the mobility of its people and resources. Urban freight and passenger demand are expected to increase at rates well above the average growth in transport. *van Aardenne et al.* [1999] and *Klimont et al.* [2001] suggest that in urban Asia, growing vehicular population and emerging technologies will have a significant

impact on transport sector emissions and in turn on the overall emissions mix. To represent this growth in the transport a third scenario was calculated, in which all the megacities had a VOC/NO_x ratio equivalent to that of Tokyo (1.5). This was achieved through varying NO_x emissions while holding the VOC emissions constant (and while holding all nonmegacity emissions to their current levels).

[52] Under this scenario, NO_x emissions were doubled in Manila, Calcutta, Dhaka, Bangkok, and Chongqing and decreased by a factor of two for Seoul, Hong Kong, and Singapore. Figure 10 shows that this scenario results in an increase in ambient O_3 levels throughout the region, with the largest increases around Seoul, Chongqing, Manila, Bangkok and the Indian subcontinent. For cities like Seoul where the photochemical activity is VOC sensitive, a decrease in NO_x emissions creates more favorable conditions for O_3 production and O_3 increases by more than 10% over the base case scenario. For cities like Chongqing, Bangkok, Calcutta, Manila, and Dhaka where the photochemical activity is NO_x limited, increases in NO_x emissions lead to increased production of O_3 (increasing the background concentrations by $\sim$5 ppbv in and around the megacities). The change in near-surface O_3 concentrations is minimal for the rest of northeast and coastal east Asia areas, which are VOC limited under current emissions.

[53] These results indicate that ozone levels may rise in large portions of Asia as a result in projected changes in NO_x and VOC emissions. However, the magnitude of the

change in the springtime is low. These results need to be repeated for different seasons in order to evaluate the robustness of these findings.

6. Summary

[54] The role of urban pollution in east and Southeast Asia as measured during the TRACE-P and ACE-Asia field experiments during the period of March–April 2001 was investigated. The emission estimates for the megacities were presented and discussed in terms of sectoral contributions and regional similarities and differences. With less than 2% of the land covered by the megacities and harboring more than 30% of Asian population, the megacities produce ~10% of the anthropogenic trace gas and aerosol emissions in Asia.

[55] A back trajectory analysis along the flight tracks was used to isolate observations points with megacity signals. A total of 1085 out of 2238 points during TRACE-P and 1457 out of 2701 points during ACE-Asia were classified to have passed over one or more of the 16 megacities included in the study, some of which were fresh urban pollution plumes out of Shanghai, Qingdao, Seoul, Pusan, Hong Kong and Tokyo. The data classified by specific megacity influence were then used to identify air mass signatures for the individual cities. For example, halon 1211 (CF_2ClBr) is a fire retardant still produced in China, and the ratios involving this species were found to be elevated in Chinese cities. CH_3Cl is a tracer for biomass and biofuel and these ratios were also elevated in Chinese cities, as were the ratios involving CCl_4 and OCS. In contrast HCFC-141b was enhanced in Japanese cities, as were the ratios involving CH_3Br. Furthermore, the BC/CO ratios were found to be highest in Tokyo, followed by Seoul, and then by the Chinese cites (all with very similar values). Comparisons of the observation-based ratios with emission-based estimates were also presented and provide a means to test for the consistency of the emission estimates. The observation-based ratios were shown to be generally consistent with the emissions ratios. Future studies that use these observation-based ratios as constraints in inverse modeling studies should provide improved estimates of megacity emissions. This is the focus of a future paper.

[56] The influence of the megacity emissions on the regional pollution distributions were studied using the STEM-2K1 regional chemical transport model, and analyzing simulations with all sources includes and those where the megacity emissions were removed. Results for specific flight days, along with monthly mean contributions were presented. Megacities contributions in excess of ~30% were found to cover regions hundreds of kilometers downwind of the major cities. The largest impacts of megacities were found over the Sea of Bengal. A megacity footprint was defined as the area where the megacity emissions account for 10% or more of the ambient pollution levels, and introduced to provide a means of discussing different species. The megacity footprint for sulfate was larger than that for SO_2, while the footprints for CO and ozone were significantly smaller than for SO_x, NO_z or HCHO.

[57] The implications of these results with respect to possible environmental futures associated with changing megacity emissions in Asia were presented. Because of the changing emission trends in Asia, the chemical conversion regimes are expected to change in the future. Model simulations exploring the sensitivity of springtime ozone to NO_x and VOC emissions (primary emissions that are expected to change dramatically in the future because of rapid motorization in the developing country cities) were performed. Most of the points associated with the megacity emissions were found to fall under "VOC limited" conditions.

[58] The megacity emission estimates provide a valuable resource for studying future emission scenarios. For example a specific simulation designed to represent growth in the transport sector, in which all the megacities have a VOC/NO_x ratio equivalent to that of Tokyo (1.5) was analyzed. The results indicate that ozone levels would rise in large portions of Asia as a result in such changes in NO_x and VOC emissions.

[59] The results presented in this paper help identify and evaluate the role of megacity emissions on air quality of the region. However, we are also left with the challenge of how to fully evaluate the impacts of megacities on regional air quality. There is no doubt that the intensity of megacity emissions has a profound negative impact on the urban scale. However, the impact on the regional scale, while noticeable, needs to be evaluated in the context of "compared to what alternative?" We presented results using one definition of a megacity footprint, designed to represent the area where megacity emissions make a disproportional contribution to air quality, and these footprints were shown to cover large regions. However, interesting questions remain. Given the same megacity emission amounts, what is the spatial distribution of sources that yields the smallest "footprint?" Are megacities an optimal way to minimize the contribution of urban emissions at regional and global scales? Clearly more work is needed to more completely assess the roles that megacities play on global and regional air quality; and we need to establish additional metrics to use in such analyses.

References

Bernsten, T., I. S. A. Isaksan, W. C. Wang, and X. Zhong (1996), Impacts of increased anthropogenic emissions in Asia on tropospheric ozone and climate, *Tellus, Ser. B*, *48*, 13–32.

Blake, N. J., et al. (2003), NMHCs and halocarbons in Asian continental outflow during the Transport and Chemical Evolution over the Pacific (TRACE-P) field campaign: Comparison with PEM-West B, *J. Geophys. Res.*, *108*(D20), 8806, doi:10.1029/2002JD003367.

Carmichael, G. R., et al. (2003a), Regional-scale chemical transport modeling in support of the analysis of observations obtained during the TRACE-P experiment, *J. Geophys. Res.*, *108*(D21), 8823, doi:10.1029/2002JD003117.

Carmichael, G. R., et al. (2003b), Evaluating regional emission estimates using the TRACE-P observations, *J. Geophys. Res.*, *108*(D21), 8810, doi:10.1029/2002JD003116.

Davis, D., A. Krupnick, and G. McGlynn (Eds.) (2001), *Ancillary Benefits and Costs of Greenhouse Gas Mitigation: Proceedings of an IPCC Co-Sponsored Workshop, held on 27–29 March 2000, in Washington, D. C.*, Org. for Econ. Coop. and Dev., Paris.

Guttikunda, S. K. (2002), Impact assessment of Asian megacity emissions on global, regional and urban air quality, Ph.D. thesis, 217 pp., Univ. of Iowa, Iowa City.

Klimont, Z., J. Cofala, W. Schopp, M. Amann, D. G. Streets, Y. Ichikawa, and S. Fujita (2001), Projections of SO_2, NO_x, NH_3, and VOC emissions in east Asia up to 2030, *Water Air Soil Pollut.*, *130*, 193–198.

Koike, M., et al. (2003), Export of anthropogenic reactive nitrogen and sulfur compounds from the east Asia region in spring, *J. Geophys. Res.*, *108*(D20), 8789, doi:10.1029/2002JD003284.

Kojima, M., C. Brandon, and J. J. Shah (2000), Improving urban air quality in south Asia by reducing emissions from two-stroke engines vehicles, report, World Bank, Washington, D. C.

Krupnick, A., and W. Harrington (2000), Energy, transportation, and environment: Policy options for environmental improvement, *ESMAP Pap. 224*, World Bank, Washington, D. C.

Mayer, M., C. Wang, M. Webster, and R. G. Prinn (2000), Linking local air pollution to global chemistry and climate, *J. Geophys. Res.*, *105*, 22,869–22,896.

Rotstayn, L. D., B. F. Ryan, and J. E. Penner (2000), Precipitation changes in a GCM resulting from the indirect effects of anthropogenic aerosols, *Geophys. Res. Lett.*, *27*, 3045–3048.

Streets, D. G., et al. (2003), An inventory of gaseous and primary aerosol emissions in Asia in the year 2000, *108*(D21), 8809, doi:10.1029/2002JD003093.

Tang, Y., et al. (2003a), Influences of biomass burning during the Transport and Chemical Evolution over the Pacific (TRACE-P) experiment identified by the regional chemical transport model, *J. Geophys. Res.*, *108*(D21), 8824, doi:10.1029/2002JD003110.

Tang, Y., et al. (2003b), Impacts of aerosols and clouds on photolysis frequencies and photochemistry during TRACE-P: 2. Three-dimensional study using a regional chemical transport model, *J. Geophys. Res.*, *108*(D21), 8822, doi:10.1029/2002JD003100.

Trainer, M., et al. (1993), Correlation of ozone within NO_y in photochemically aged air, *J. Geophys. Res.*, *98*, 2917–2925.

Uno, I., et al. (2003a), Regional chemical weather forecasting system CFORS: Model descriptions and analysis of surface observations at Japanese island stations during the ACE-Asia experiment, *J. Geophys. Res.*, *108*(D23), 8668, doi:10.1029/2002JD002845.

Uno, I., G. R. Carmichael, D. Streets, S. Satake, T. Takemura, J. Woo, M. Uematsu, and S. Ohta (2003b), Analysis of surface black carbon distributions during ACE-Asia using a regional-scale aerosol model, *J. Geophys. Res.*, *108*(D23), 8636, doi:10.1029/2002JD003252.

van Aardenne, J. A., G. R. Carmichael, H. Levy, D. G. Streets, and L. Hordijk (1999), Anthropogenic NO_x emissions in Asia in the period 1990–2020, *Atmos. Environ.*, *33*, 633–646.

Woo, J.-H., et al. (2003), Contribution of biomass and biofuel emissions to trace gas distributions in Asia during the TRACE-P experiment, *J. Geophys. Res.*, *108*(D21), 8812, doi:10.1029/2002JD003200.

Yienger, J. J., M. K. Galanter, T. A. Holloway, M. J. Phadnis, S. K. Guttikunda, G. R. Carmichael, W. J. Moxim, and H. Levy II (2000), The episodic nature of air pollution transport from Asia to North America, *J. Geophys. Res.*, *105*, 26,931–26,945.

————————————

G. R. Carmichael and L. Pan, Department of Chemical and Biochemical Engineering, University of Iowa, Iowa City, IA 52242, USA. (gcarmich@engineering.uiowa.edu)

A. Fried, National Center for Atmospheric Research, Boulder, CO 80303, USA.

S. K. Guttikunda, Environment Department, World Bank, Washington, DC 20433, USA.

G. Kurata, Y. Tang, and N. Thongboonchoo, Center for Global and Regional Environmental Research, University of Iowa, Iowa City, IA 52242, USA.

D. G. Streets, Decision and Information Sciences Division, Argonne National Laboratory, Argonne, IL 60439, USA.

J.-H. Woo, Northeast States for Coordinated Air Use Management, Boston, MA 02114, USA.

Figure 2. Contribution of various sectors to total urban and regional primary pollutant emissions in Asia in 2000: IND, industry; PG, power generation; TRAN, transportation; DOMF, domestic fossils; DOMB, domestic biofuels; BB, biomass burning.
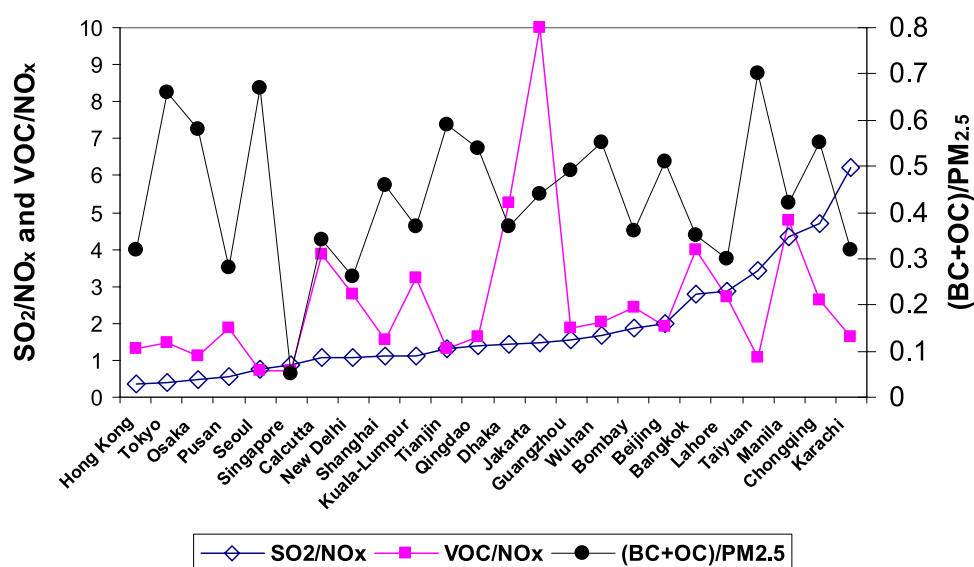
Figure 3. Primary trace gas and aerosol emission ratios (by weight) for the megacities in Asia in 2000.
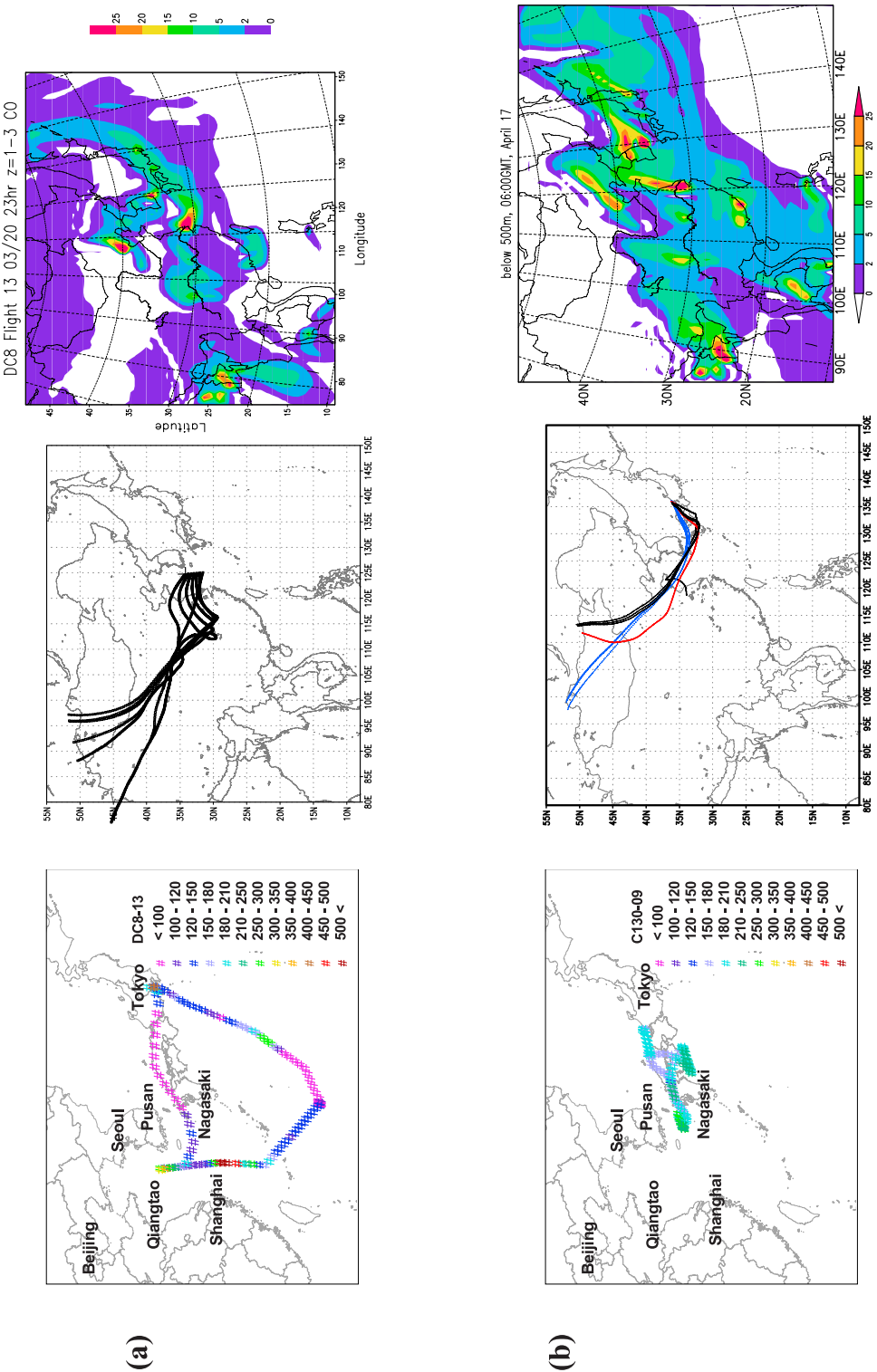
Figure 4. Identification of megacity signals using flight path with CO measurements, back trajectories, and percent contribution of megacity emissions to pollutant mixing ratios during the flight operation averaged between 0 and 500 m. (a) TRACE-P DC8-09 flight path, back trajectories between 0500 and 0530 GMT, and percent contribution to CO mixing ratios. (b) ACE-Asia C130-09 flight path with CO measurements, back trajectories between 0400 and 0500 GMT, and simulated percent contribution to CO mixing ratios.

(a)

(b)

Figure 5. Statistics from backward trajectory analysis of all the measurement points along the (a) TRACE-P DC8 and P3 flight tracks and (b) ACE-Asia C-130 flight tracks. Color code indicates expected age of the trajectory from the city of origin when intercepted (in days).
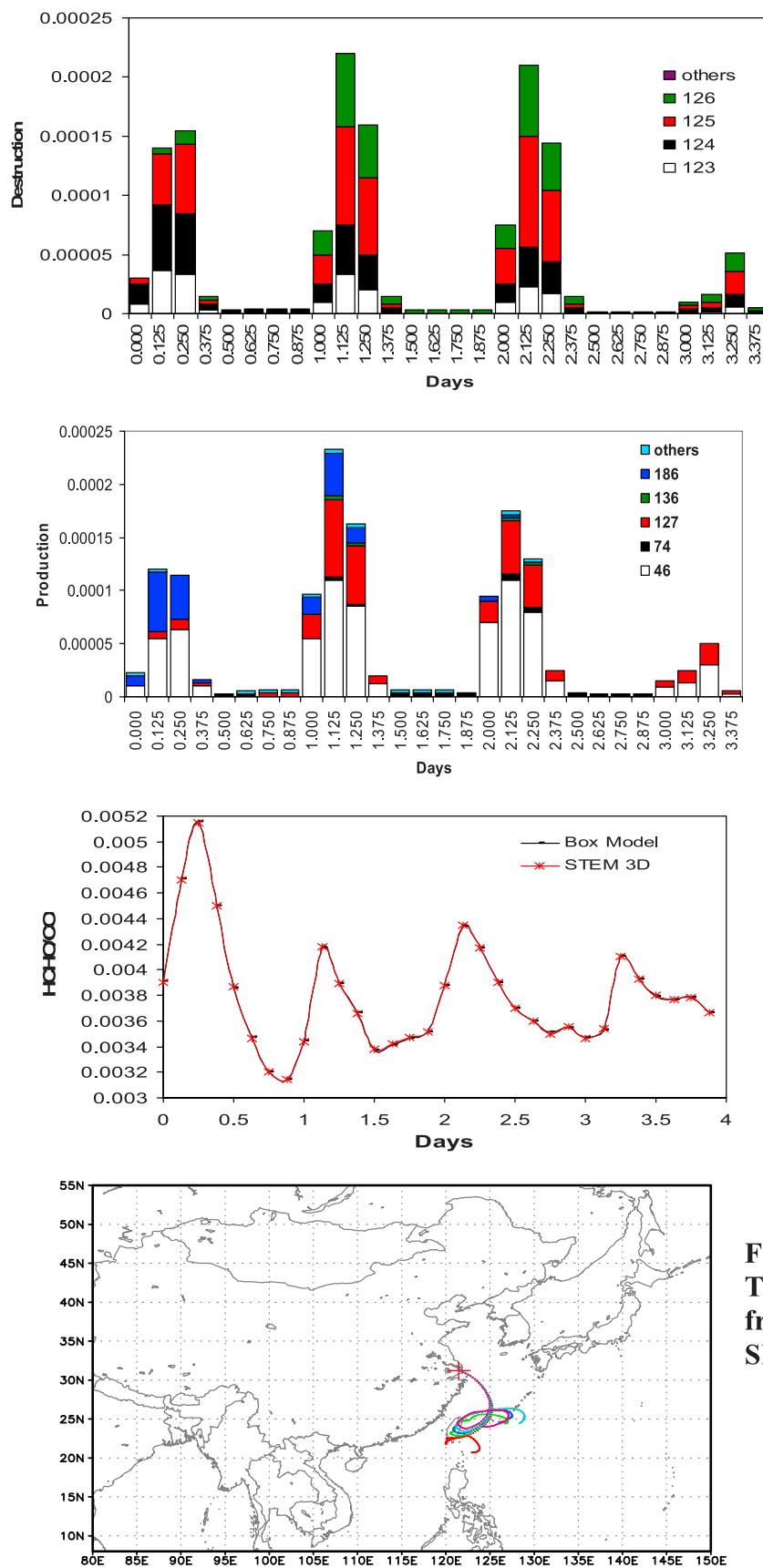
Figure 8

Figure 8. Calculated HCHO/CO along the path of a forward trajectory originating from Shanghai on 17 March (Julian day 76) at 0100 GMT. Destruction and production pathways are also shown. The related reactions are (46) $C\_O_2 + NO \rightarrow NO_2 + HCHO + HO_2$, (74) $CCO\_O_2 + C\_O_2 \rightarrow CH_3COOH + HCHO$, (123) $HCHO + hv \rightarrow 2HO_2 + CO$, (124) $HCHO + hv \rightarrow CO$, (125) $HCHO + OH \rightarrow HO_2 + CO$, (126) $HCHO + HO_2 \rightarrow HOCOO$, (127) $HOCOO \rightarrow HO_2 + HCHO$, (136) $ACETONE + OH \rightarrow HCHO + CCO\_O_2 + R_2O_2$, and (186) $ETHENE + OH \rightarrow RO_2\_R + 1.61HCHO + 0.195CH_3CHO$. Here C_O_2 represents methyl peroxy radicals; CCO_O_2 represents acetyl peroxy radicals; HOCOO is the radical formed when HCHO reacts with HO_2; and RO_2_R and R_2O_2 are the peroxy radical operators representing NO to NO_2 conversion with and without HO_2 formation, respectively.
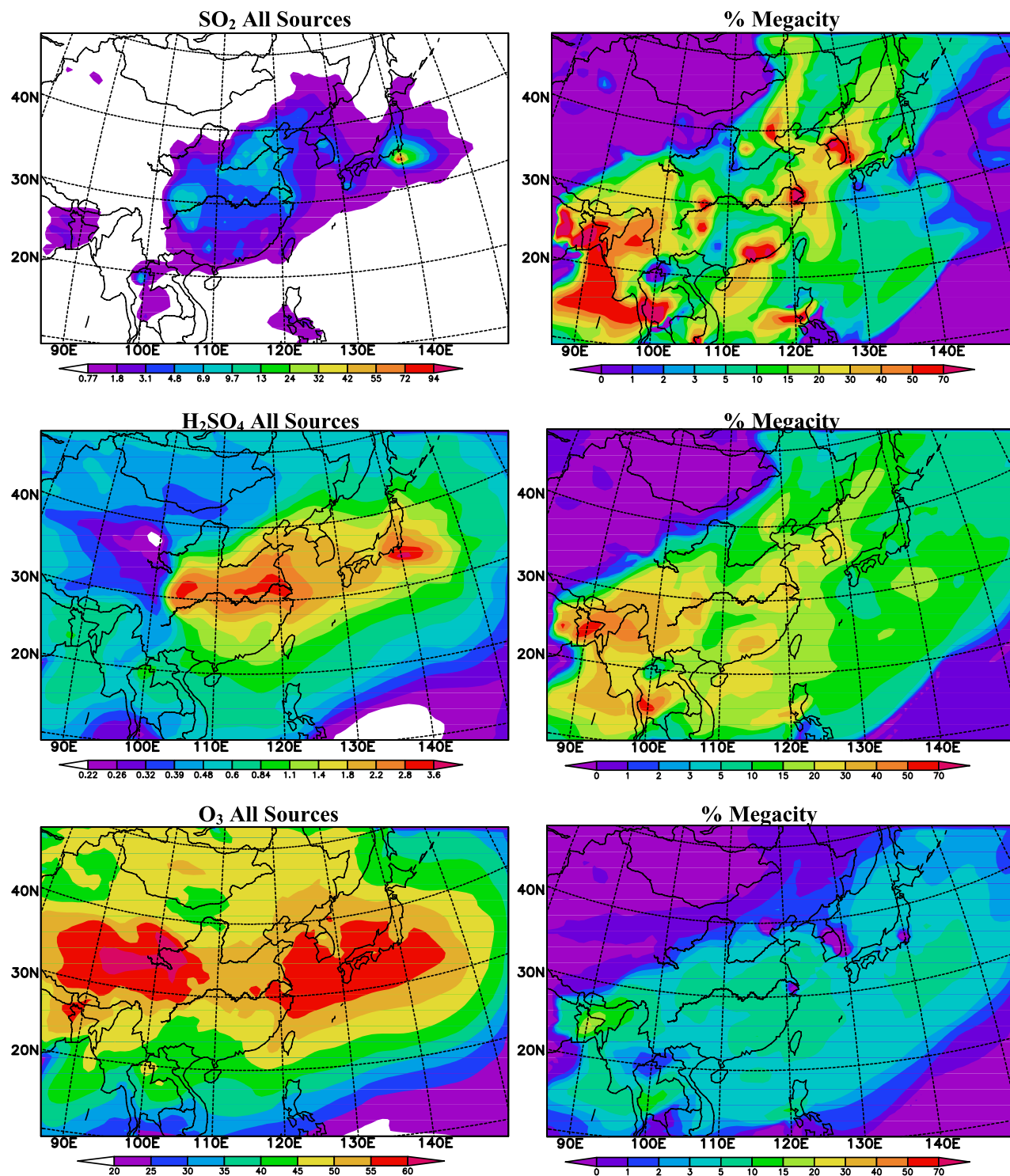
Figure 9. Simulated monthly average mixing ratios (ppbv) with all the anthropogenic and biomass sources included and percentage contribution of Asian megacity emissions averaged below 1 km during the period of March 2001.
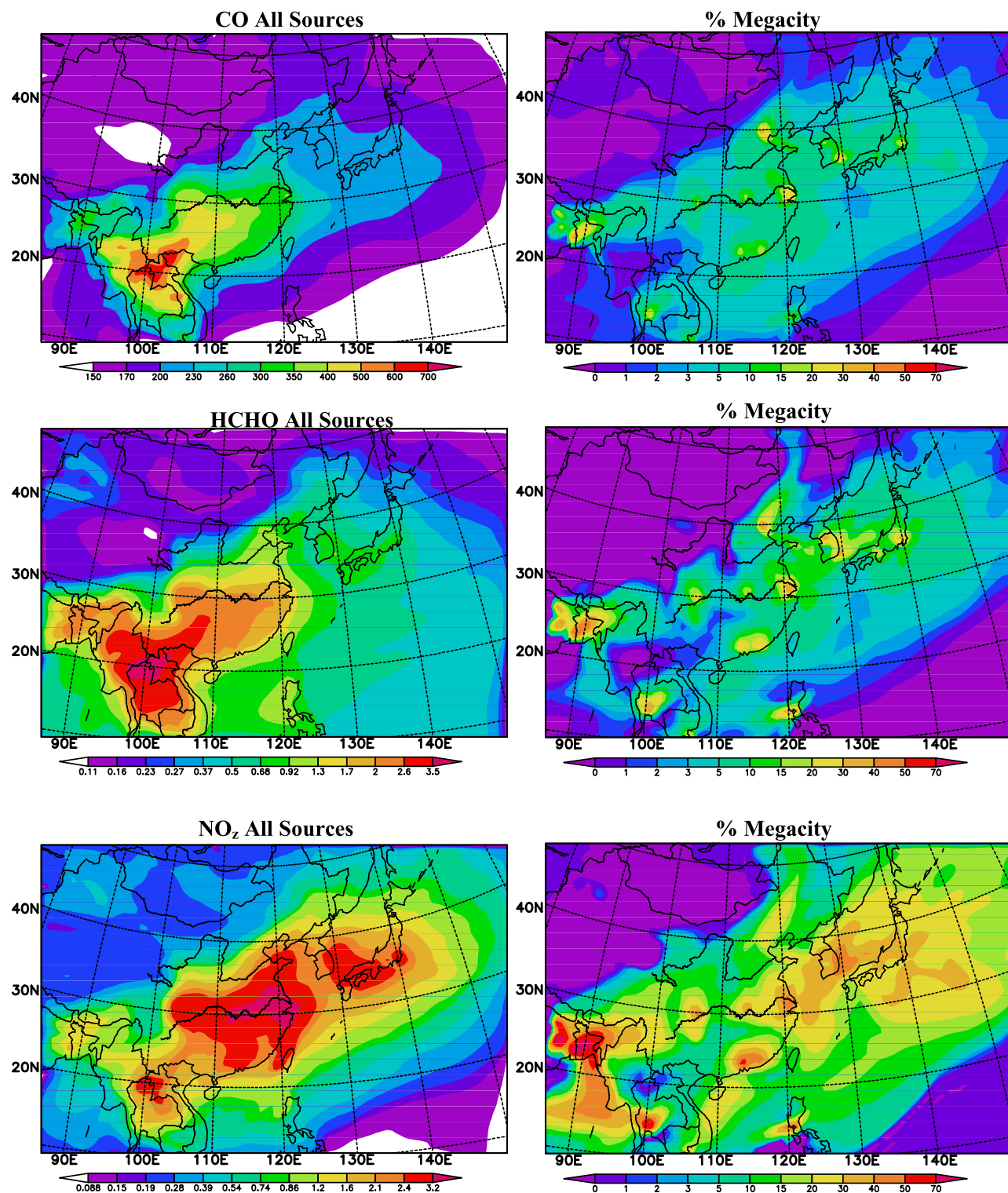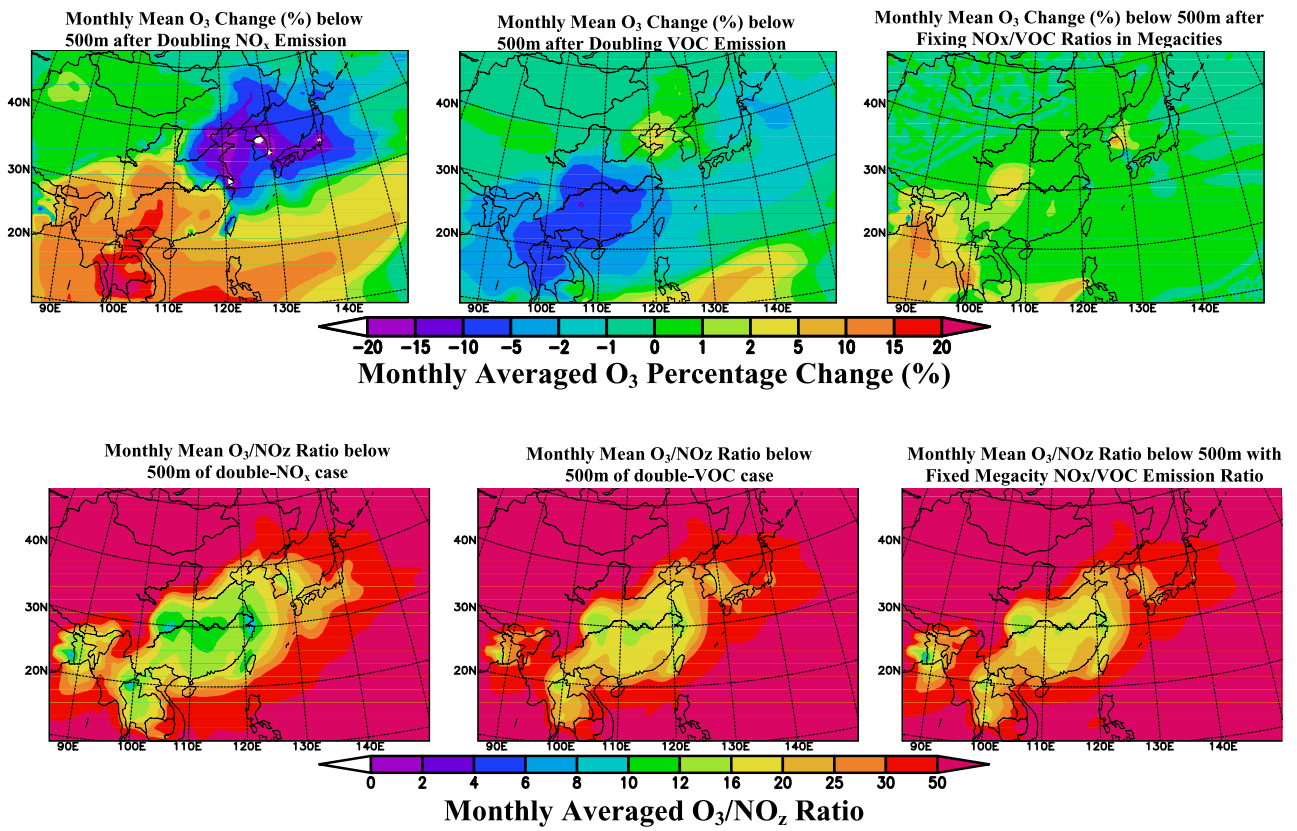
Figure 9. (continued)

Figure 10. Percentage change in monthly average O_3 concentrations and ratio of monthly average O_3 to NO_z mixing ratios upon doubling of NO_x and VOC emissions below 500 m.